UNIVERSITY OF SALERNO

DEPARTMENT OF INDUSTRIAL ENGINEERING

Ph.D. Course in Industrial Engineering
Curriculum in Mechanical Engineering - XXXIII Cycle

Design of a non-invasive system for real-time monitoring of driver's drowsiness and fatigue through the analysis of cardiac signals

Supervisor
Prof. Arcangelo Pellegrino

Ph.D. student
Luca Salvati

Scientific Referees
Prof. Miryam Liliana Chaves Acero
Prof. Carlo Cattani

Ph.D. Course Coordinator
Prof. Francesco Donsì

A.A. 2021-2022

Design of a non-invasive system for real-time monitoring of driver's drowsiness and fatigue through the analysis of cardiac signals

Luca Salvati

UNIVERSITY OF SALERNO

DEPARTMENT OF INDUSTRIAL ENGINEERING

Ph.D. Course in Industrial Engineering
Curriculum in Mechanical Engineering - XXXIII Cycle

Design of a non-invasive system for real-time monitoring of driver's drowsiness and fatigue through the analysis of cardiac signals

Supervisor
Prof. Arcangelo Pellegrino

Ph.D. student
Luca Salvati

Scientific Referees
Prof. Miryam Liliana Chaves Acero
Prof. Carlo Cattani

Ph.D. Course Coordinator
Prof. Francesco Donsì

Acknowledgements

I would like to gratefully thank Prof. Arcangelo Pellegrino and Prof. Francesco Villecco for the endless support, moral as well as professional, given during the PhD path. In them I appreciated the passion for the profession, humanity and my esteem and gratitude go to them. I also thank Dr. Pasquale Sena to whom I owe the ability to develop a critical and visionary approach towards specific research topics, my witty officemate Damiano Fortuna for the significant contribution to my personal and professional improvement and Eng. Mario Pisaturo for the invaluable support during this experience.

Many thanks to my beloved family (Fortunata, Carmine, Andrea, Angela, Francesca) who have constantly supported me in the choices and in the moments of remoteness.

List of contributions

Publications on international peer reviewed journals

- Salvati, L.; d'Amore, M.; Fiorentino, A.; Pellegrino, A.; Sena, P.; Villecco, F. Development and Testing of a Methodology for the Assessment of Acceptability of LKA Systems. Machines 2020, 8, 47. https://doi.org/10.3390/machines8030047
- Salvati, L.; d'Amore, M.; Fiorentino, A.; Pellegrino, A.; Sena, P.; Villecco, F. On-Road Detection of Driver Fatigue and Drowsiness during Medium-Distance Journeys. Entropy 2021, 23, 135. https://doi.org/10.3390/e23020135
- Salvati, L.; Cappetti, N.; d'Amore, M.; Fiorentino, A.; Pellegrino, A.; Sena, P.; Villecco, F. Heart Sound Processing Model for a Mat-Shaped Device (accepted and pending publication)
- Salvati, L.; d'Amore, M.; Fiorentino, A.; Pellegrino, A.; Sena, P.; Villecco, F. HRV analysis through the processing of the sphygmic wave pulsation acquired by a sensor in the proximity of the femoral artery (under examination)

Summary

List of Figures

List of Tables

Abstract

The development and spread of human-centered products that are increasingly simple and affordable has seen their application areas increase over the years, as well as their effectiveness and reliability. Real-time monitoring physiological conditions, such as fatigue and sleepiness, offers useful support in both clinical and driving safety fields and it is essential in accident prevention. This research proposes a detection platform without direct contact with the skin capable of acquiring cardiac signals and it develops a fatigue-related sleepiness detection algorithm based on the analysis of the pulse rate variability generated by the heartbeat and validates the proposed method by comparing it with an objective indicator of sleepiness (PERCLOS). Changes in alert conditions affect the autonomic nervous system (ANS) and therefore heart rate variability (HRV), modulated in the form of a wave and monitored to detect long-term changes in the driver's condition using real-time control. The performance of the algorithm was evaluated through an experiment carried out in a road vehicle. In this experiment, data was recorded by 3 participants in different driving sessions and their conditions of fatigue and sleepiness were documented on both a subjective and objective basis. The validation of the results through PERCLOS showed a 63% adherence to the experimental findings. The present study confirms the possibility of continuously monitoring the driver's status through the detection of the activation/deactivation states of the ANS based on HRV. The proposed method can help prevent accidents caused by drowsiness while driving.

Introduction

One of the priorities of current approaches in automotive research is to help the driver avoid accidents. Human error is the main cause of fatalities on the road, due to lack of attention or excess fatigue. Therefore, a strategy for coping with this problem is to detect how the driver is feeling at all times by monitoring his activities.

Monitoring of driver behavior and the reliable detection of sleepiness and fatigue is one of the main objectives in the development of new ADAS concepts. Nowadays, most of the sleep detection systems on the market are based on the control of driving performance. These techniques evaluate the variables recorded by the CAN, such as the position of the vehicle in the lane, its speed and the movements of the steering wheel. Some research groups have also used techniques based on eye and head movement (Nagai, 2008; Dikkers, 2004), and there are also methods based on biomedical signals, such as brain, muscle and cardiovascular activity (Oron-Gilad, 2008; Papadelis, 2007; Faber, 2004), although most of them are still far from actually being introduced to the market, according to recent surveys (Wright, 2007).

Approaches based on biomedical signals are particularly useful for monitoring changes in the body's state during the sleep cycle. The information they provide goes beyond the usual systems that detect only risky circumstances (degraded driving performance or visual symptoms of lack of attention) and can potentially predict the onset of sleepiness. The main disadvantage of techniques based on biomedical signals is that they would require the positioning of sensors directly on the body: although there have already been some attempts to record them indirectly, through non-intrusive systems (Lee H.B., 2007; Lee B.G., 2011), they do not always manage to guarantee a continuity of the detection due to loss or degradation of physical or visual contact at the sensor/user interface.

Cardiac activity is an important and easy-to-measure indicator of the driver's status. There are several techniques to measure it, but electrocardiography (ECG) is the most direct and informative. Cardiac activity varies according to the person's activity, and lack of attention can be identified by analyzing heart rate variability (HRV). A person focused on doing an activity usually exhibits a more regular heart rate, and as the focus on activity

decreases, the heart rate becomes more irregular and HRV increases (Oron-Gilad, 2008).

Fatigued drivers show changes in the way their eyes perform certain actions, such as moving or blinking. These actions are known as visual behaviors and are easily observed in sleepy drivers. The percentage of eye closure (PERCLOS) was found to be the most reliable indicator of sleepiness (Dinges, 1998).

Some camera-based systems that attempt to assess the driver's status by recognizing facial expressions only work well in ideal circumstances (head straight and face forward) (Dikkers, 2004; Lenskiy, 2012), but they are very sensitive to glasses, head movements and lighting conditions.

Many techniques for drowsiness detection have been proposed. Sensors in the seat have been proposed to monitor the seat pressure or the driver's pulse wave [Juki, 2014]. However, its introduction cost is high. Another method is to detect deterioration of the vestibulo-ocular reflex (VOR), which is a sign of drowsiness (Nishiyama, 2010). However, it is difficult to monitor VOR in a dark environment because it relies on image analysis.

Regardless of the type of measurement, one of the main problems with sleepiness detection studies is the difficulty of performing experimental tests to validate the techniques.

For safety reasons, experimental tests for the sleepiness detection are often conducted on driving simulators, in laboratories with a controlled environment and with the possibility of using measuring devices that are difficult to integrate into real vehicles.

However, the main limitations of laboratory experiments are their low realism and the risk of simulator sickness (Bos, 2008), as well as the alteration of the spontaneous behavior of drivers: sleepiness is reliably caused by a combination of the accumulated fatigue of the driver and boredom associated with monotonous activity, especially on familiar roads and vehicles. The unusual experience of participating in such an experiment, especially when the subjects are equipped, or the "white coat effect" due to the presence of researchers, can hinder sleepiness; or conversely, the higher level of stimulation in real road conditions can reduce sleepiness (Akerstedt, 2005). These conditions affect the effectiveness of the experiments and therefore the development of reliable models for detecting sleepiness: for this reason it is necessary to have a balanced and realistic quantity of detections on subjects both during periods of wakefulness and sleepiness.

This study illustrates the evolution in the design of a recognition model of the physiological states of the individual starting from the acquisition of the cardiac signal, passing through the interpretation of its characteristic parameters in the time and frequency domain, to finally arrive at the definition of a scheme that allows that model to be expressed in the forms of drowsiness and fatigue.

Chapter I
Principles of Physiology

I.1 The cardiovascular system

The cardiovascular system is a closed and continuous system with high pressure portions and low pressure parts. The left ventricle (Figure I.1) throws blood into the aorta which then distributes it through the distinct body regions using a network of vessels. The aorta (as well as the pulmonary arteries on the right), in addition to being the main distribution vessel, also has the function of transforming intermittent flow into continuous flow thanks to its high elastic component. The large arteries (carotid, mesenteric and renal) branch off from the aorta and distribute blood to specific organs. From these arteries, smaller and smaller vessels branch off and enter the organs to supply them (Figure I.2).

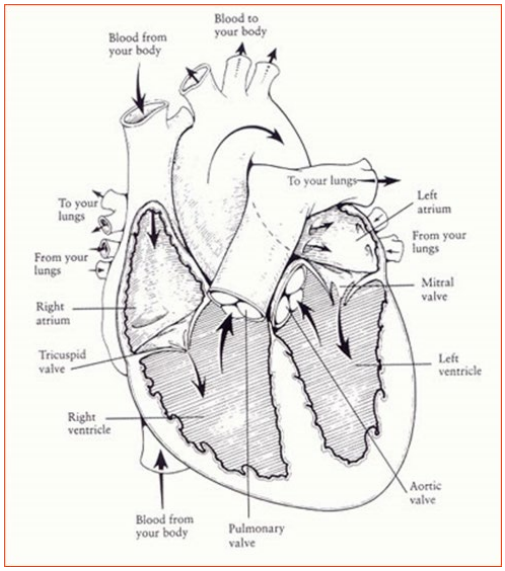

Figure I.1 *Conduction system of the heart*

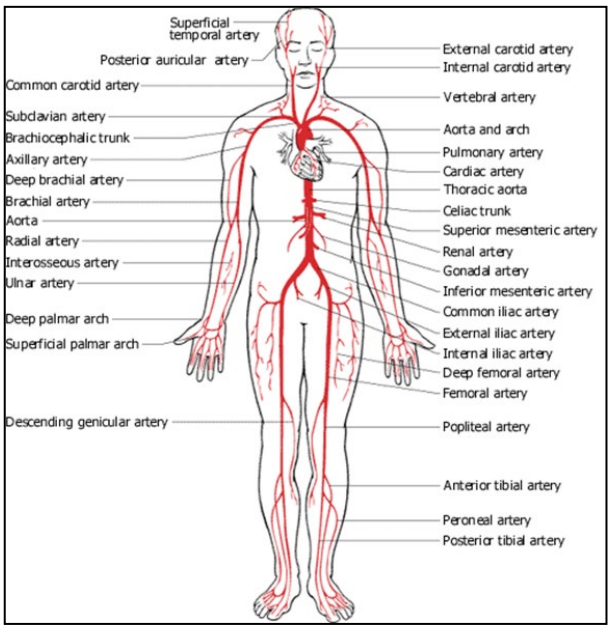

Figure I.2 *Schematic of the cardiovascular system*

The arterioles, richly innervated by the autonomic nervous system, are entrusted with the task of regulating the local flow. The capillaries, on the other hand, have the function of exchanging oxygen, carbon dioxide, water, electrolytes, proteins, metabolic substrates and hormones. Veins have a capacitive function of harboring blood.

I.2 Sphygmic wave: theoretical principles

The motion of the blood is determined by the activity of the heart. This activity is characterized by the rhythmic and regular succession of a contraction phase of the ventricular muscles called systole (during which a certain amount of blood is pushed from the ventricles into the arteries) followed by a phase called diastole (during which the ventricles are released filling again with the blood coming from the atria and reaching them through the venous vessel system).

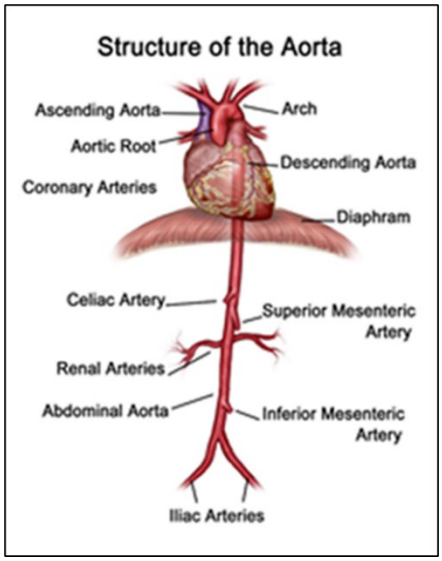

Figure I.3 *Structure of the Aorta*

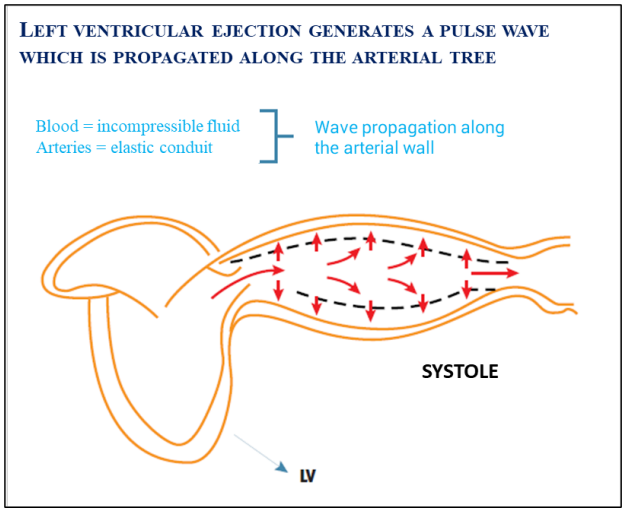

Figure I.4 *Left ventricular ejection*

At each systole the arteries, in particular the aorta (Figures I.3-4), thanks to the elasticity of their wall, dilate to accommodate the blood that comes from the heart, and then they return, during diastole, to the previous conditions. This rhythmic dilation of the arterial wall begins at the origin of the aorta and then it spreads like a wave (sphygmic wave, Figure I.5) along all the arteries. With its passage it determines that phenomenon commonly called "pulse", that is, the pulsation that is felt with palpation on any accessible artery and which is generally detected on the radial artery in the wrist region. The sphygmic wave

propagates in the various arteries with different speed, which increases from the center towards the periphery: on average it is 5-8 m/s (speed much greater than that of the blood flow), so the radial pulse is felt 0.1 s after the peak of cardiac systole. This speed is essentially related to the elasticity of the arterial wall: it increases as the latter decreases, so in elderly subjects it is significantly increased due to vascular sclerosis. The rhythmic dilation of the arterial wall also has the effect of making the blood flow continuous, which is pumped into the arterial circulation in a discontinuous manner, that is, only during cardiac systole. During diastole the arterial wall, due to its elasticity, retracts and returns to itself, and thus it pushes the blood towards the small peripheral vessels. Therefore the blood flow in the large arteries has an oscillating character, which gradually decreases as it proceeds towards the small arteries, until it disappears completely in the capillaries. The flow velocity also varies as it proceeds from the aorta towards the periphery. In fact, by considering blood vessels as a system of rigid tubes, the velocity of a liquid inside them depends, at each point, on the total cross section of the vessel bed in those points: since the total section of the capillary bed has a surface area of 1000 times ca. wider than that of a section of the aorta, at that level there will be a very significant reduction in flow velocity. This one has an average value of 40 cm/s in the aorta (from 120 cm/s during systole, up to a negative value in diastole, when a transient retrograde flow occurs before the aortic valves close); in small-caliber arteries the flow velocity is always greater during systole, but it is more continuous and directed forward; in the capillaries the flow is continuous, and its speed is reduced to a few mm / s and even less (Bompiani, 1990).

In other words, the energy consumed by the ventricle during contraction is transferred to the aorta generating two different wave phenomena that propagate along the arterial tree: a flow wave, which proceeds at low speed (about 1 m/s in aorta) and is attenuated by proceeding from the center towards the periphery, and a pressure wave or sphygmic wave, which proceeds at a much higher speed (typically 4-8 m/s in the normal aorta) and which has different and completely peculiar characteristics.

We are used to expressing the sphygmic wave in a given point of the arterial tree as the change in blood pressure that occurs during a cardiac cycle, that is, in terms of systolic and diastolic blood pressure. However, an obvious characteristic of the pressure in the arterial tree, yet neglected for decades in both clinical practice and research, is that it is a wave, that is, a periodic oscillatory movement that travels from the heart to the peripheral arteries.

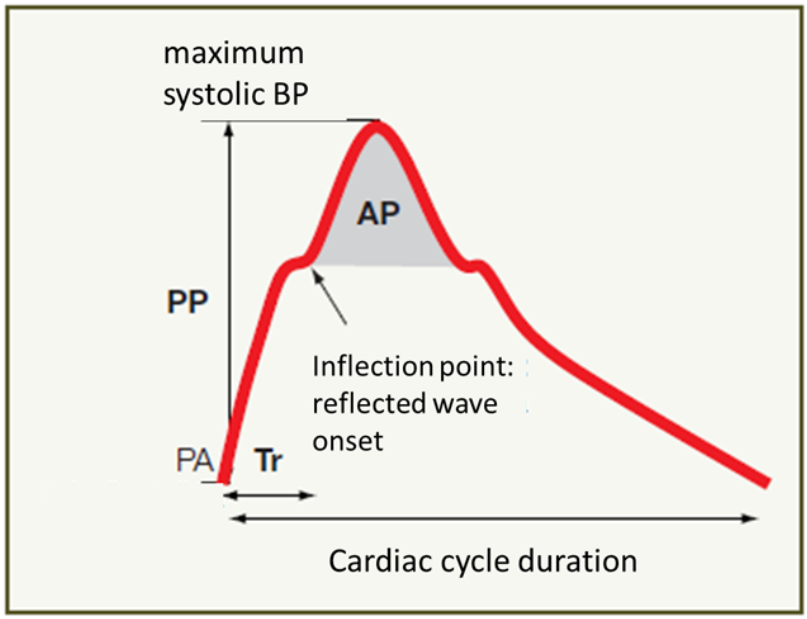

Figure I.5 *Sphygmic wave in the aorta analyzed in the time domain. The wave amplitude corresponds to the differential pressure (pulse pressure, PP), and the frequency to the ratio: 1 / duration of the cardiac cycle. Tr indicates the interval between the arrival of the incident wave and the arrival of the reflected wave. AP (augmentation pressure) represents the increase in the sphygmic wave due to the reflected wave*

The nature of this oscillation can be understood if it is compared to another wave with well-known characteristics, such as the acoustic wave. Similarly to the acoustic wave, the pulse wave:

1) it can be reflected and amplified;

2) it has an amplitude and a frequency;

3) it can be analyzed by breaking it down over time (time domain analysis) or its sinusoidal harmonic components (frequency domain analysis).

At each point of the arterial tree, the shape of the sphygmic wave is the result of the incident wave (which travels from the center to the periphery) and the reflected wave. Reflections of the sphygmic wave occur at the level of multiple sites in which there are changes in arterial properties (eg, elasticity, stiffness, vasomotor tone) or due to the architecture of the arterial tree (e.g., bifurcations, calcifications). The reflection site is not really a single physically distinct site, but rather a statistical notion: the multiple waves reflected by the various sites merge into a single reflected wave, which is added to the incident wave and thus forms the final sphygmic wave (Bramwell, 1922; Avolio, 2009).

I.3 Electrocardiography: ECG signal

One of the most important problems in the measurement of biomedical signals is represented by the presence of disturbances and noise that contaminate the signal of interest, preventing a correct determination of its trend. The top graph of Figure I.6 illustrates a noise-contaminated ECG signal. The use of filtering techniques allows to reduce or eliminate the noise level present in the signal and to obtain a "cleaned" signal. Ultimately, the filtering operation allows a more precise and accurate recognition of the QRS complex that characterizes the ECG signal (graph at the bottom of Figure I.6).

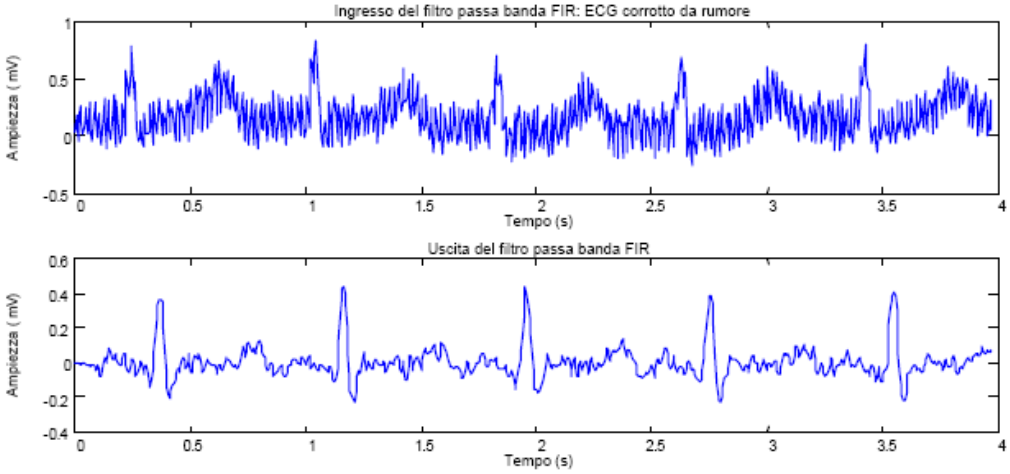

Figure I.6 *Noise-contaminated ECG signal (top), filtered ECG signal (bottom)*

The characteristic parameters that can be extracted from an ECG are numerous, first of all the temporal distance between the two R-R peaks of successive beats, on whose value the calculation of the Heart Rate (HR) is based (Figura I.7).

In a healthy organism there is a dynamic balance between the sympathetic nervous system (SNS) and the parasympathetic nervous system (PNS), the two branches of the autonomic nervous system. PNS activity prevails at rest.

The heart rate calculated at a specific time represents the net effect of the neural response of the parasympathetic nerves, which slow down HR, and of sympathetic nerves, which accelerate it. In the literature, this mechanism is referred to as an “antagonistic” mechanism.

The normal sinus rhythm of the resting heart is highly irregular during steady-state conditions. The change in time intervals between adjacent beats is called Heart Rate Variability (HRV).

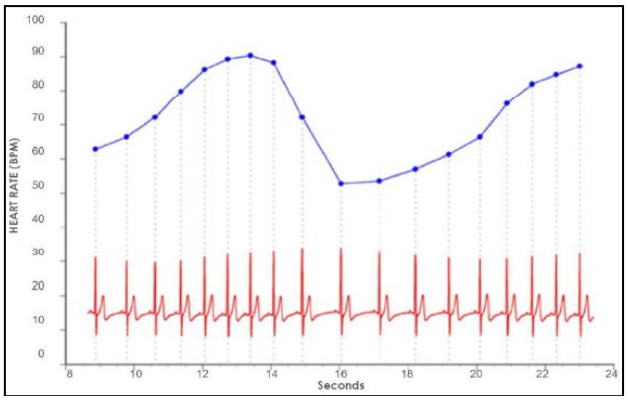

Figure I.7 *ECG and Heart Rate*

These fluctuations in heart rate are the result of complex and non-linear interactions between different physiological systems (autonomic nervous system, blood pressure, and respiratory control systems) in response to conditioning factors (stress, drowsiness). The most common modality of observing these changes is the so-called tachogram, the graph of a sequence of time intervals between the R peaks (Figura I.8). A reduced HRV can be predictive of future heart problems because it reflects a reduced ability to regulate, which is the ability to respond adequately to exercise or stress situations.

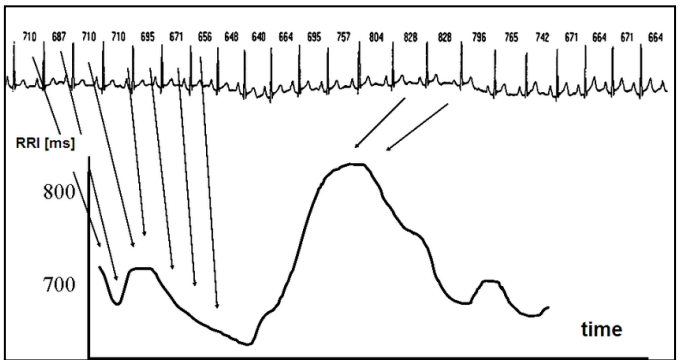

Figure I.8 *Tachogram*

I.4 Heart Rate Variability

Every individual finds himself having to daily face various physiological and environmental stimuli, which subject his organism to a perennial effort of adaptation. In this regard, the Autonomous Nervous System (ANS) assumes a fundamental role, since it highlights the person's ability to adapt and conform:

it acts, in fact, as a sort of "orchestra conductor" regulating all physiological processes, both in normal homeostatic as well as pathological conditions, through the alternation of excitatory (sympathetic system) and inhibitory (parasympathetic system) actions.

In order to determine the psycho-physical health of an individual, a promising and non-invasive technique for evaluating the sympathetic and parasympathetic functions of the ANS has spread in recent decades: Heart Rate Variability (HRV). The effectiveness and immediacy of the results, the ease of data acquisition and processing, without neglecting the accessibility of the cost, are the reasons for the success of this new evaluation procedure.

A high variability of the heart rhythm is an indirect signal of the good degree of adaptation to internal and external stimuli and it characterizes a healthy individual with efficient mechanisms of regulation of the ANS. On the contrary, a low variability of the heart rhythm is often an indication of abnormal and insufficient adaptation to external factors with consequent reduced physiological function of the individual. By analyzing the result of an HRV analysis, it is also possible to determine the prevalence of sympathetic or parasympathetic activity and how much, in a situation of imbalance, the activity of one of these two nervous systems prevails over the other one (Malik, 1996).

In order to establish univocal criteria for reading and interpreting the parameters obtained from a HRV analysis, in 1996 the Task Force of the European Society of Cardiology and the North American Society of Pacing Electrophysiology established guidelines, which are still valid today and internationally followed.

Historically, his clinical interest emerged in 1965 when Lee S. T. detected the presence of alterations in the R-R intervals of the ECG signal recorded to monitor fetal distress. Subsequently, other authors (Luczak, 1973; Hirsch, 1981) focused their attention on the existence of physiological rhythms inserted in the heart rate signal, until in 1977 the HRV took hold in cardiology, proving to be a reliable index of mortality risk in patients who had suffered acute myocardial infarction (Wolf, 1977).

Over the years, in addition to witnessing an increase in the applications of this technique in the cardiology field, its effectiveness and reliability have also been demonstrated in other application areas, including psychology, psychiatry, psychotherapy and, the latest arrivals in chronological terms, sports medicine and wellness, with the spread of increasingly accessible and easy-to-use instruments, up to the recent integration in numerous smartphones.

I.5 HRV analysis

Heart rate is defined as the average number of heart beats per minute. Actually, the time that passes between a heartbeat and the next one is not constant, but it changes continuously (Laurin, 2013; Tadi, 2015).

Each of us has a natural variability of heart rate in response to factors such as breathing rhythm, emotional states, anxiety, stress, anger, relaxation, thoughts, etc. In a healthy heart, the heart rate responds quickly to all these factors, changing according to the situation, so that the body is able to adapt as well as possible to the different needs that the environment continually submits to us. A healthy individual shows a good degree of heart rate variability, which translates into a good degree of psychophysical adaptability to the different situations that may arise.

The study of Heart Rate Variability (HRV) consists in the measurement and analysis of heartbeat variations, in order to deduce some important information in the diagnosis of various clinical and functional conditions or for daily health monitoring (Montano, 2009; Pumprla, 2002; Porges, 1995). It is also the main tool available for the non-invasive evaluation of the dynamics of ANS, in terms of balancing the activity between the sympathetic and parasympathetic nervous systems (sympathetic/vagal balance), and it reflects the homeostatic interaction between the disturbances in the central cardiovascular system functions and the dynamic responses of cardiovascular regulatory systems (Malik, 1996; Porges, 2003).

In particular, the Sympathetic Nervous System, when activated, produces a series of effects such as: acceleration of the heartbeat, dilation of the bronchi, increase in blood pressure, peripheral vasoconstriction, pupillary dilation, increased sweating. The Sympathetic system is the body's normal response to a situation of alarm, struggle, stress.

On the contrary, the Parasympathetic Nervous System (also called Vagal Activity), when activated, produces a slowing of the heart rhythm, an increase in bronchial muscle tone, dilation of blood vessels, decrease in pressure, slowing of breathing, increased muscle relaxation, breathing becomes calmer and deeper. The Parasympathetic System represents the body's normal response to a situation of calm, rest, tranquility and the absence of dangers and stress. Our body, at all times, is in a situation determined by the balance or the predominance of one of these two nervous systems.

The body's ability to change its balance towards one or the other system is very important and it is a fundamental mechanism which tends to the dynamic balance of the organism both from a physiological and psychological point of view. Hence the great importance of having today a scientific instrument such as HRV capable of evaluating the relative state of the Sympathetic and Parasympathetic nervous system.

HRV signals are usually calculated by analyzing a time series of beat-to-beat intervals measured by electrocardiography (ECG) or derived from a pulse

wave signal that is measured using a photoplethysmography sensor (PPG waveform) applied to a finger, which detects the cyclical variations of the pressure tone in the capillaries of the finger itself, which faithfully represent the heartbeat. Once digitized, the data is analyzed by software that calculates the R-R distance (expressed in milliseconds, ms) between one heartbeat and the next and it creates a diagram, based on the number of heartbeats, the so-called tachogram.

Then the software performs further more complex analyzes, i.e. the Resampling of the tachogram, the Fourier Transform and the calculation of the Power Spectrum of the tachogram (expressed in ms^2), which represents the frequency components of the tachogram and it contains the essential information to arrive at the aforementioned estimate of the balance between Sympathetic and Parasympathetic. The power spectrum (in the frequency domain) expresses the power of the frequencies between 0.01 and 0.4 Hz (Clifford, 2005).

I.5.1 Methods of HRV analysis

The study of HRV focuses mainly on the analysis in the time and frequency domain (Cerutti, 1995; Kleiger, 1995; Litvack, 1995; Malik, 1996). However, cardiac activity is an integrated signal that is influenced not only by the two branches of the ANS, but also by a number of other subordinate physiological mechanisms and various external factors.

I.5.1.1 Time domain analysis

Time domain measures are basically divided into two classes: (a) measures of variability derived from RRI data; (b) measures of variability derived from the differences between adjacent RRIs. To the first subclass belong the mean RRI (mRRI), the HR and the standard deviation of the RRI (SDNN), immediate but also the least informative. In the second subclass, the most explanatory parameter is undoubtedly the RMSSD: it is used to estimate the high frequency beat-to-beat variations that represent vagal regulation activity. A low rMSSD value indicates poor parasympathetic activity and difficulty in recovering from physical exertion or from a situation of high emotional stress. Other parameters used to assess beat-to-beat variations include NN50, the number of adjacent RRIs that differ by more than 50 ms, and pNN50 (NN50/total number of RRIs). Since these parameters are highly correlated with RMSSD, they are also good estimators of vagal activity (von Borell, 2007).

I.5.1.2 Geometric analysis

The Poincaré map (Lorenz diagram) is the scatter plot of the intervals between beats as a function of the previous intervals between beats (Karmakar, 2010). It is a geometric technique originating from non-linear dynamics (Brennan, 2001; Golińska, 2013).

I.5.1.3 Spectral analysis of HRV by FFT

The FFT technique is applied only to equidistant sampled series, therefore the raw HRV time series must be converted to equidistant sampled series by interpolation methods before the FFT analysis (Cerutti, 1995). The LF/HF ratio is defined as the ratio of power in the LF band to power in the HF band (Malik, 1996).

In the frequency domain, three sub-bands of frequencies can be distinguished within this spectrum:

- VLF (Very Low Frequency): frequencies between 0.01 and 0.04 Hz. The VLF band is due in part to the activity of the Sympathetic Nervous System, by changes in thermoregulation, and in the psychological field it is influenced by worries and obsessive thoughts (worry and rumination).
- LF (Low Frequency): frequencies between 0.04 and 0.15 Hz. The LF band is considered mainly due to the Sympathetic Nervous System and the regulation of the baroreceptors.
- HF (High Frequency): frequencies between 0.15 and 0.4 Hz. The HF band is considered an expression of the activity of the Parasympathetic Nervous System. This frequency zone is highly influenced by the rhythm and depth of breathing.

The FFT technique allows you to assign power in different bands to different underlying physiological functions. It is widely accepted that the power in the HF band represents vagal activity (Malliani, 1994; Akselrod, 1995; Houle, 1999), while the LF and VLF bands are associated with sympathetic activity or sympathetic plus vagal activity, and their physiological significance has been much debated (Ponikowski, 1996; Yeragani, 2002) (Figura I.9).

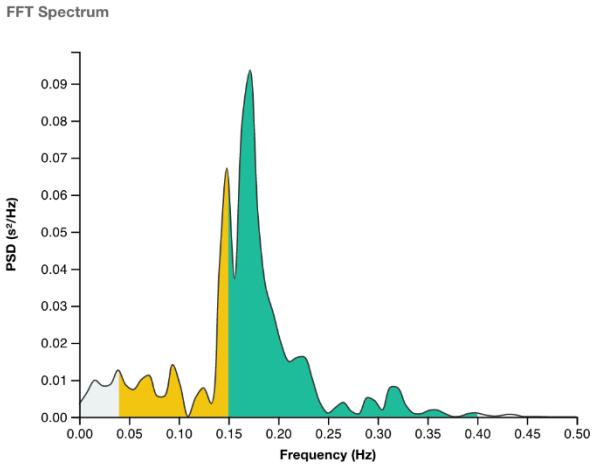

Figura I.9 *Power Spectrum*

I.5.1.3.1 LF and HF power bands

There are four main frequency bands of heart rhythms: high frequency (HF), low frequency (LF), very-low frequency (VLF) and ultra-low frequency (ULF). The first two classes characterize phenomena and processes that develop over minutes or tens of minutes; on the contrary, phenomena in the VLF and ULF bands require longer recordings to emerge (as the timing of the experiments examined in this study).

The HF power (0.15÷0.4 Hz) reflects the parasympathetic or vagal activity and it is often called the *breathing band* because it corresponds to changes in heart rate related to the respiratory cycle: the HR accelerates during inspiration and slows down during exhalation. The power LF (0.04 ÷ 0.15 Hz) reflects the resting activity of the baroreceptors, i.e. the neurosensory receptors that respond to pressure changes in the cardiovascular system.

The LF/HF ratio can be interpreted as a sympatho-vagal index: in fact, since the HF band reflects the activity of the only parasympathetic system, while the LF band takes into account both the sympathetic and the parasympathetic ones, a decrease of this ratio is generally seen as an imbalance towards the parasympathetic activity, while its increase is an indication of an imbalance towards the sympathetic activity.

Since emotional, attentional and stress responses also involve the autonomic nervous system (in addition to the central nervous system) they can be associated with changes in HRV and in particular with changes in the sympathetic-vagal balance. For example, in conditions of increased workload (stress conditions) there is an increase in heart rate, and an increase in the LF/HF ratio.

Chapter II
Heart Sound

II.1 Heart sound processing model for a mat-shaped device

The development and spread of Human-centered products is based on satisfying the user's needs mainly related to performance, interaction, comfort and usability. This design concept finds application in product development in the industrial sector: the diffusion of increasingly accessible and easy-to-use instruments, their application in the most diverse fields, is the context from which this study of a model able to provide support for research in both clinical and purely commercial fields was born. A technology based on the acquisition and processing of biosignals, in this case the cardiac ones, allows the search for physiological parameters capable of providing an objective reading of perceptual states related to the sensations of fatigue, malaise and postural discomfort, concentration and sleepiness, as well as define the product ergonomic performance.

As mentioned above HRV analysis is useful in assessing the dynamics of the autonomic nervous system (ANS) and detecting the effects of numerous systemic diseases as well as changes related to the normal daily biological rhythm or to accidental situations of stress or fatigue, as well as comfort or vigilance.

Therefore, the study of a model based on the interpretation of cardiac signal is able to provide real-time monitoring of physiological conditions and to offer useful support in both medical and driving safety fields.

The developed model allows for the acquisition of the heart's vibro-acoustic signal, that can be subjected to HRV analysis at a later stage thanks to the compiled algorithm.

II.1.1 Detection system

This section describes the procedure for detecting the heartbeat acquired through a sensor integrated into a mat placed on the back of a seat at a height close to that of the heart (about 40 cm from the seat). To detect the HR and

the characteristic HRV indices, an algorithm was developed that can identify the R peaks of the ECG wave by processing the heart sound signal coming from the seated subject. This signal is recorded through a capacitive microphone sensor embedded in a specific support made of 3D polyester material and inserted into a mat (Figure II.1).

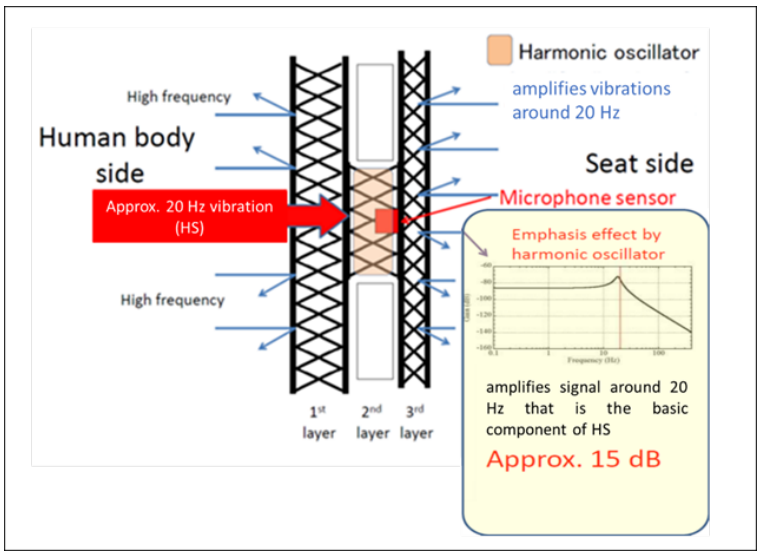

Figure II.2 *Layer structure of the sensing system*

This fabric approximates the elastic characteristics of muscles in a relaxed state, having almost the same load-displacement characteristics as human skin (Kojima 2015) and it acts as an oscillator with a center frequency of approximately 20 Hz and, through the phenomenon of stochastic resonance, allows the filtering of the acoustic signal around 20 Hz for the removal of artifacts (Hagiyama, 2018, 2019; Salvati, 2021).

The frequency range of the microphone developed to capture heart sounds is 30 to 70 Hz, which is the frequency band of heart sounds. This microphone can measure sounds from 0,1 Hz, but it has high sensitivity in the 10 to 30 Hz frequency range.

The acquisition of cardiac signals, both from ECG and from sensor, takes place at a sampling rate of 1000 Hz.

II.1.2 Signal Processing

In order to eliminate the noise components due to breathing or movement artifacts, three types of bandpass filter with different cut-off frequencies were tested to recognize which produced the cardiac signal most similar to that obtained with the electrocardiograph. Therefore for the first bandpass filter (b.p.f) the frequency bands 10-30 Hz, 15-80 Hz and 4-50 Hz were chosen and

subsequently the signal was filtered between 0.8 and 1.8 Hz so that it assumed the analogous wave form to an electrocardiographic signal, having a frequency close to 1 Hz (Figure II.2). The evaluation of the time interval between the peaks of this waveform allows an estimate of the parameters in the time and frequency domain typical of HRV analysis (Figure II.3).

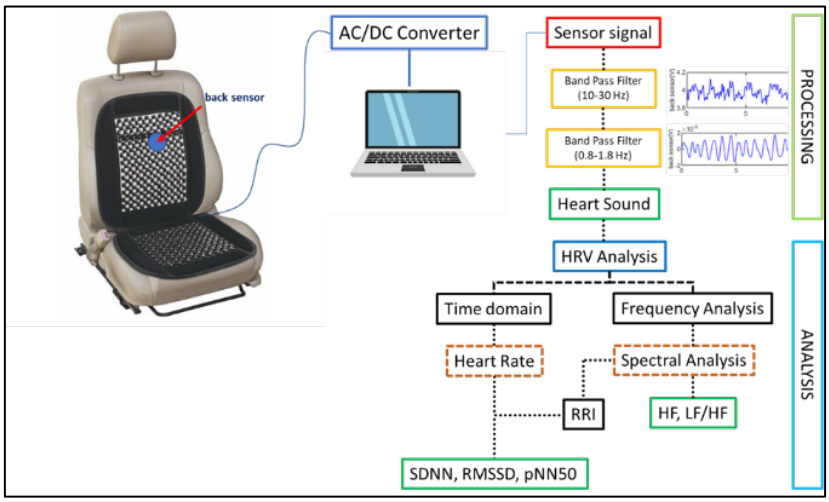

Figure II.2 *Signal processing*

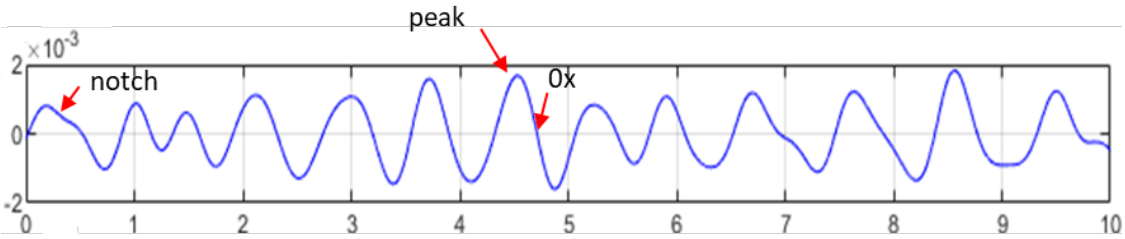

Figure II.3 *Heart sound waveform*

II.1.3 Experimental Protocol

Ten healthy subjects between the ages of 25 and 54 were made to sit for 5 minutes on a car seat fixed on the floor of the laboratory and equipped with the mat that incorporates the sensor. Participants were asked to sleep at least 7 hours the night before the experiment, not to smoke and not to take caffeine, alcohol or energy drinks after waking up until the time of the experiment. The subjects were also asked to arrange the three ECG electrodes on themselves. The electrodes were placed in RA (right arm), LA (left arm) and LL (left leg) positions (Figure II.4).

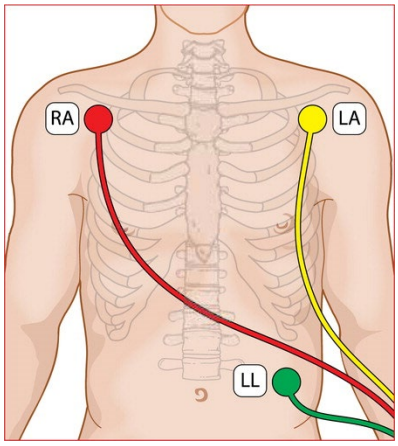

Figure II.4 *Placement of ECG electrodes*

II.1.4 Results

A preliminary visual examination of the Poincaré Plot, relating to both the ECG signal and the heart sound (HS) signal processed by the algorithm, revealed that no signal loss was recorded during the detection (Figure II.5).

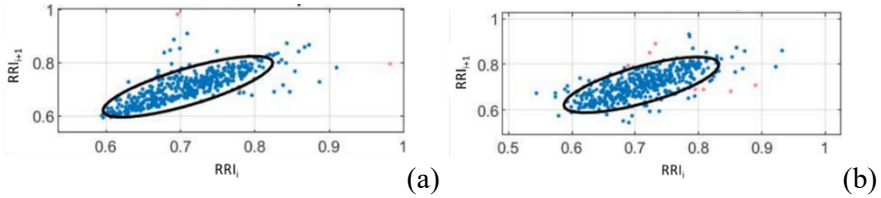

(a) (b)

Figure II.5 *(a) RRI Poincaré Plot; (b) HS peaks Poincaré Plot*

To establish which filter offered the best performance, the tachograms of the ECG and HS signals relating to each acquisition were compared. A Pearson correlation coefficient "r" was calculated for each comparison. Then the average relative to the analyzes carried out with the same b.p.f. was calculated. And the most performing filter turned out to be the one with a frequency range of 10-30 Hz, as shown in Table II.1.

Table II.1 *Comparison of b.p.f. filters*

	Pearson correlation coefficient r		
	10-30 Hz	15-80 Hz	4-50 Hz
Subjects	r	r	r
1	0.78	0.89	0.28
2	0.68	0.18	0.17
3	0.62	0.56	0.47
4	0.30	0.31	0.22
5	0.38	0.37	0.15
6	0.34	0.58	0.47
7	0.43	0.25	0.15
8	0.52	0.14	0.44
9	0.68	0.31	0.37
10	0.63	-0.19	0.20
Mean	0.54	0.34	0.29

Subsequently, the measurements obtained with the sensor that showed the greatest and least correspondence with the tachogram obtained from the ECG are reported, respectively those of Subject 1 and Subject 4. With regard to Subject 1, in Figure II.6 the trend of the tachogram obtained from the HS signal (red line) reproduces with good approximation the trend of the RRI obtained from the ECG, so much that even the parameters in the time domain HR, RRI, SDNN, RMSSD, SD1, SD2 are equal or deviate by a few units (Table II.2) (Fig II.7).

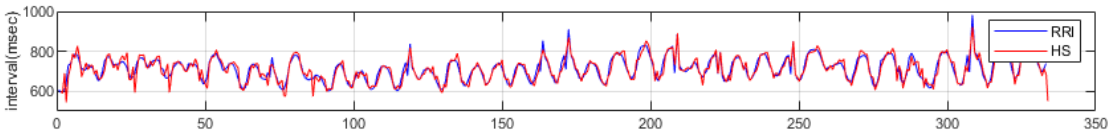

Figure II.6 *Subject 1: overlap of the tachogram obtained with ECG (HR) and sensor (HS)*

Table II.2 *Comparison of cardiac parameters in the time domain (Subject 1)*

	ECG	HS
Mean RR | HR	709 | 85	709 | 85
SDNN	58.7	61.4
RMSSD	44.6	45.2
pNN50	11.7	21.6
SD1 | SD2	31.5 | 76.5	31.9 | 80.5
SD1/SD2 ratio	0.41	0.4

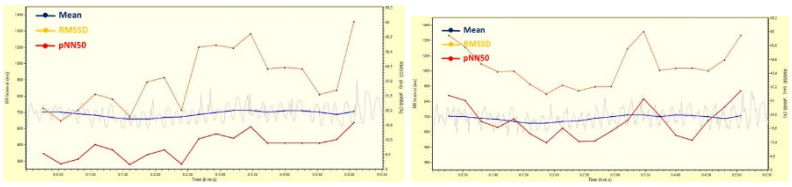

Figure II.7 *mRRI, RMSSD, pNN50 variations in the time domain (Subject 1)*

To further appreciate the similarity of the results obtained, an analysis in the frequency domain was also performed. Figure II.8 shows the time course of the HF and LF/HF parameters for both ECG acquisition and sensor one: from a visual estimate it can be seen that in this case the algorithm can only approximate the actual LF/HF trend and it works better on the HF signal. The spectral diagram in Figure II.9 certainly offers a quantifiable estimate of the algorithm's efficiency.

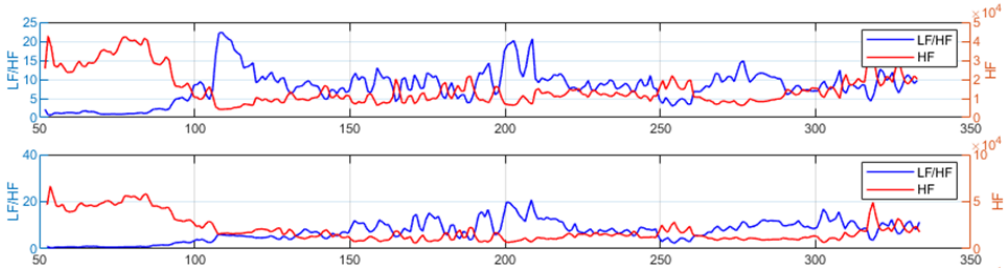

Figure II.8 *Subject 1's HRV Frequency Analysis: comparison between ECG (top) and sensor (bottom) results*

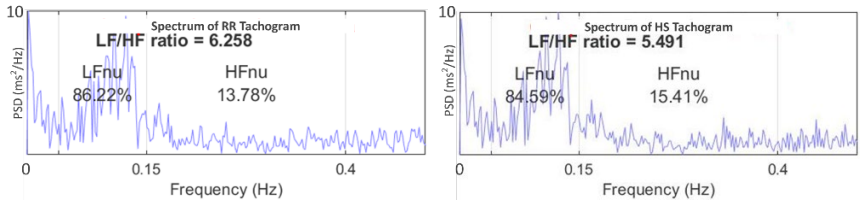

Figure II.9 *Subject 1: spectral analysis of the RR tachogram from ECG and HS signals*

By observing the results obtained on Subject 4, it can be seen that the algorithm still manages to offer a good interpretation of the heart signal, however failing to provide close reproduction in all time segments (Figure II.10).

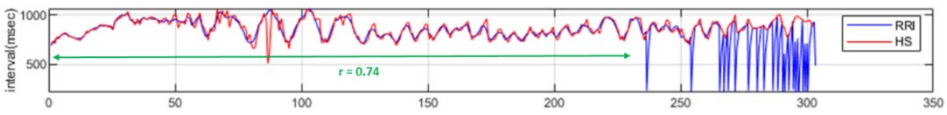

Figure II.10 *Subject 4: overlap of the tachogram obtained with ECG (HR) and sensor (HS)*

This loss of correct information is inevitably transferred to the calculation of the typical parameters of the HRV, as it is evident from the extent of the deviations between the values shown in Table II.3 and Fig II.11.

Table II.3 *Comparison of cardiac parameters in the time domain (Subject 4)*

	ECG	HS
Mean RR | HR	860 | 70	857 | 70
SDNN	79.0	84.8
RMSSD	35.9	56.2
pNN50	13.4	34.1
SD1| SD2	25.4 | 108.5	39.7 | 112.5
SD1/SD2 ratio	0.23	0.35

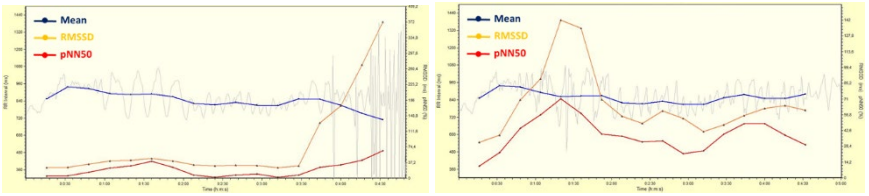

Figure II.11 *mRRI, RMSSD, pNN50 variations in the time domain (Subject 4)*

At such low correlation values, even the frequency analysis becomes unreliable (Figures II.12-13).

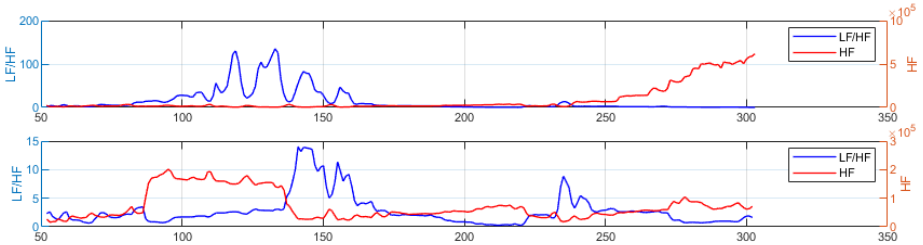

Figure II.12 *Subject 4's HRV Frequency Analysis: comparison between ECG (top) and sensor (bottom) results*

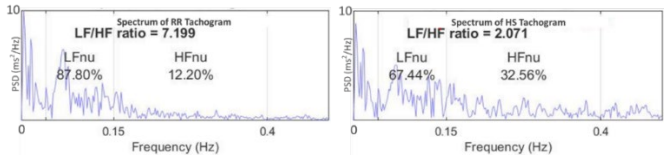

Figure II.13 *Subject 4: spectral analysis of the RR tachogram from ECG and HS signals*

All performances are validated through comparison with a clinic device. Even if this tool does not present the practicality of wearable models, it certainly offers the possibility of accessing more accurate information than what an average user or sportsman needs. The potential offered by such a system in both the clinical and commercial fields is considerable: the possibility of continuous monitoring of health state or a remote homecare service are just some of the prospects, as well as monitoring in real-time states of stress, fatigue and drowsiness of a driver or defining new applicable comfort indices in ergonomic and postural studies. The non-invasiveness of this device is a breakthrough. However, the susceptibility of the results of such a device still represents a limit and above all it would be necessary to increase the number of tests in order to understand the source of these interpretative errors which appear suddenly and therefore could be attributed to movement artifacts or anomalies such as ectopic beats.

II.2 HRV analysis through the processing of the sphygmic wave pulsation acquired by a sensor in the proximity of the femoral artery

In this study, the HRV parameters obtained from the analysis of the data acquired through an electrocardiograph were compared with those ones obtained from the use of a non-invasive system consisting of a sensor, incorporated in a cushion on which the subject is seated, able to detect the pulsations produced by the sphygmic wave (SWP) also through clothing.

II.2.1 Detection system

During the tests carried out in the previous experiment, a cushion of the same fabric as the mat was placed on the seat and an identical sensor was integrated inside it. The latter was placed slightly to the left, halfway between the spinal termination of the coccyx and the transit point closest to the femoral artery.

The developed algorithm was able to identify the peaks of the wave generated by the sphygmic pulsation through the processing of the vibrational signal coming from the seated subject.

This signal is recorded through a capacitive microphone sensor embedded in a specific support made of 3D polyester material and inserted into a cushion. This material acts as an oscillator with a center frequency of approximately 20 Hz and, through the phenomenon of stochastic resonance, allows the filtering of the acoustic signal around 20 Hz for the removal of artifacts (Hagiyama, 2018, 2019; Salvati, 2021).

The acquisition of cardiac signals, both from ECG and sensor, takes place at a sampling rate of 1000 Hz.

II.2.2 Signal Processing

In order to eliminate the noise components due to movement artifacts, three types of bandpass filter with different cut-off frequencies were tested to recognize which produced the most similar signal to that obtained with the electrocardiograph. Therefore for the first bandpass filter (b.p.f.) the frequency bands 10-30 Hz, 15-80 Hz and 4-50 Hz were chosen and subsequently the signal was filtered between 0.8 and 1.8 Hz so that it assumed the analogous waveform to an ECG signal, having a frequency close to 1 Hz. The evaluation of the time interval between the peaks of this waveform allows an estimate of the parameters in the time and frequency domain typical of HRV analysis (Figura II.14).

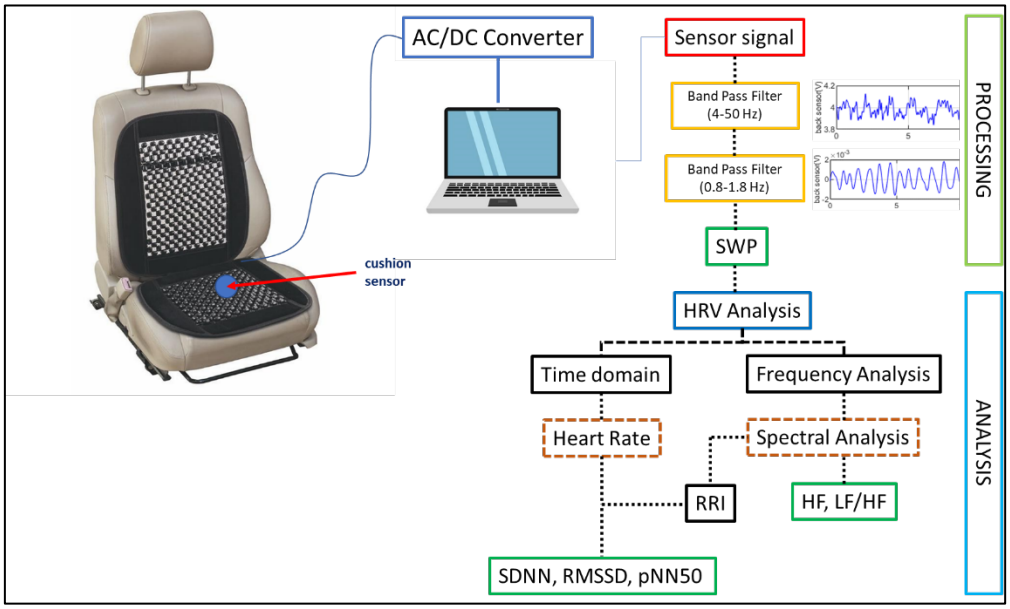

Figure II.14 *Signal processing*

II.2.3 Results

To establish which filter offered the best performance, the tachograms of the ECG and SWP signals relating to each acquisition were compared. A Pearson correlation coefficient "r" was calculated for each comparison. Then the average relative to the analyzes carried out with the same b.p.f. was calculated. and the most performing filter turned out to be the one with a frequency range of 4-50 Hz, as shown in Table II.4.

Table II.4 *Comparison of b.p.f. filters*

	Pearson correlation coefficient r		
	10-30 Hz	15-80 Hz	4-50 Hz
Subjects	r	r	r
1	0.62	0.58	0.65
2	0.21	0.04	0.45
3	0.33	0.82	0.54
4	0.48	0.21	0.46
5	0.31	0.51	0.38
6	0.53	0.90	0.55
7	0.69	0.93	0.94
8	0.35	0.62	0.35
9	0.28	0.50	0.42
10	0.20	-0.21	0.56
Mean	0.40	0.49	0.53

Subsequently, the measurements obtained with the sensor that showed the greatest and least correspondence with the tachogram obtained from the ECG are reported, respectively those of Subject 7 and Subject 8. With regard to Subject 7, in Figure II.15 the trend of the tachogram obtained from the SWP signal (red line) reproduces with good approximation (r=0.94) the trend of the RRI obtained from the ECG and HR, RRI, SDNN parameters in the time domain are very close to the actual ones (Table II.5) (Fig II.16).

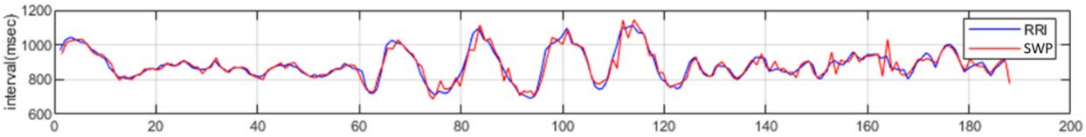

Figure II.15 *Subject 7: overlap of the tachogram obtained with ECG (HR) and sensor (SWP)*

Table II.5 *Comparison of cardiac parameters in the time domain (Subject 7)*

	ECG	SWP
Mean RR | HR	877 | 68	876 | 69
SDNN	86.3	83.9
RMSSD	39.8	52.3
pNN50	17.4	28.1
SD1 | SD2	28.1 | 118.8	37.0 | 112.9
SD1/SD2 ratio	0.24	0.33

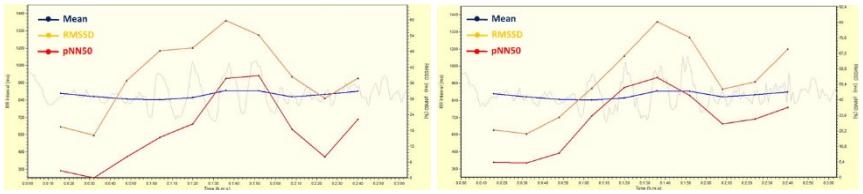

Figure II.16 *mRRI, RMSSD, pNN50 variations in the time domain (Subject 7)*

A visual examination of the Poincaré Plot, relating to both the ECG signal and the SWP signal processed by the algorithm, revealed that no signal loss was recorded during the detection (Figure II.17).

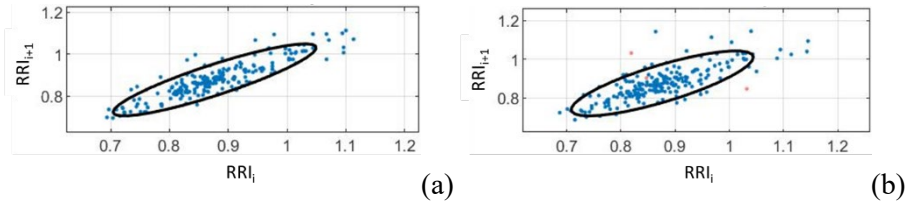

Figure II.17 *Subject 7: (a) RRI Poincaré Plot; (b) SWP peaks Poincaré Plot*

To further appreciate the similarity of the results obtained, an analysis in the frequency domain was also performed. Figure II.18 shows the time course of the HF and LF/HF parameters for both ECG acquisition and sensor one: from a visual estimate it can be seen that in this case the algorithm can only approximate the actual LF/HF trend and it works better on the HF signal. The spectral diagram in Figure II.19 certainly offers a quantifiable estimate of the algorithm's efficiency.

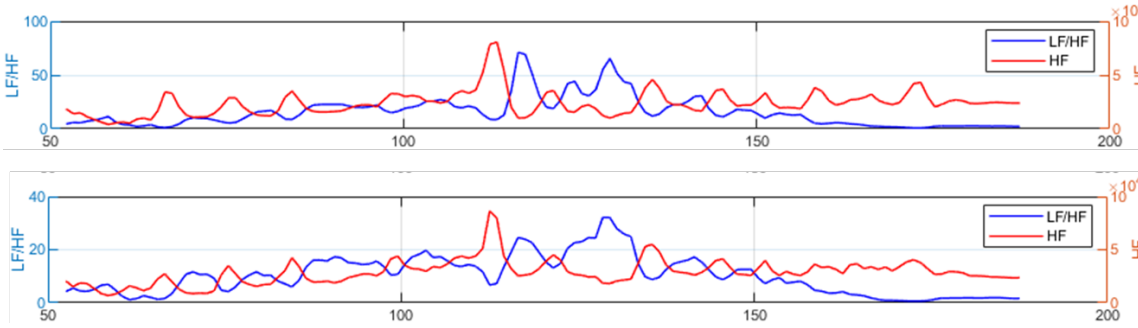

Figure II.18 *Subject 7's HRV Frequency Analysis: comparison between ECG (top) and SWP (bottom) results*

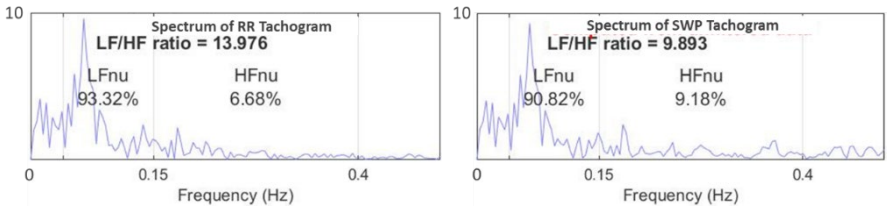

Figure II.19 *Subject 7: spectral analysis of the RR tachogram from ECG and SWP signals*

By observing the results obtained on Subject 8, it can be seen that the algorithm manages to offer an inconspicuous (r=0.35) interpretation of the heart signal, while managing to follow its trend (Figure II.20).

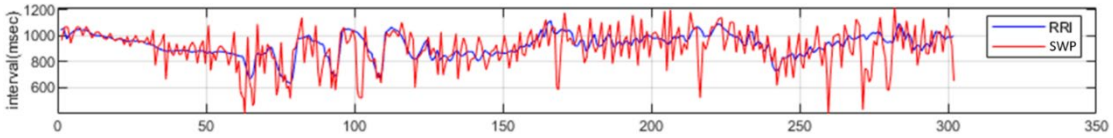

Figure II.20 *Subject 8: overlap of the tachogram obtained with ECG (HR) and sensor (SWP)*

This loss of correct information is inevitably transferred to the calculation of the typical parameters of the HRV, as it is evident from the extent of the deviations between the values shown in Table II.6 and Fig II.21.

Table II.6 *Comparison of cardiac parameters in the time domain (Subject 8)*

	ECG	HS
Mean RR | HR	921 | 65	903 | 66
SDNN	93.0	139.4
RMSSD	42.7	121.5
pNN50	14.7	64.0
SD1| SD2	30.2 | 128.0	85.9 | 165.4
SD1/SD2 ratio	0.24	0.52

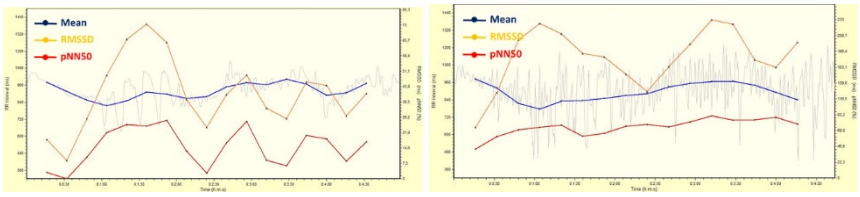

Figure II.21 *mRRI, RMSSD, pNN50 variations in the time domain (Subject 8)*

A visual examination of the Poincaré Plot, relating to both the ECG signal and the SWP signal processed by the algorithm, revealed that no signal was missed during the detection (Figure II.22).

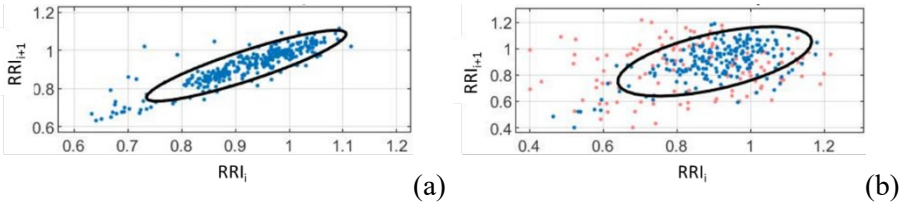

(a) (b)

Figure II.22 *Subject 8: (a) RRI Poincaré Plot; (b) SWP peaks Poincaré Plot*

Even if the correlation value was low, the frequency analysis shows a similarity in the trend of the LF/HF ratio throughout the survey and of the HF parameter only in the second half. (Figures II.23-24).

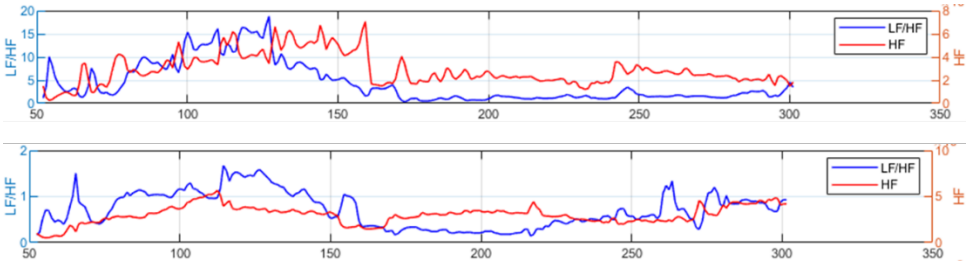

Figure II.23 *Subject 8's HRV Frequency Analysis: comparison between ECG (top) and SWP (bottom) results*

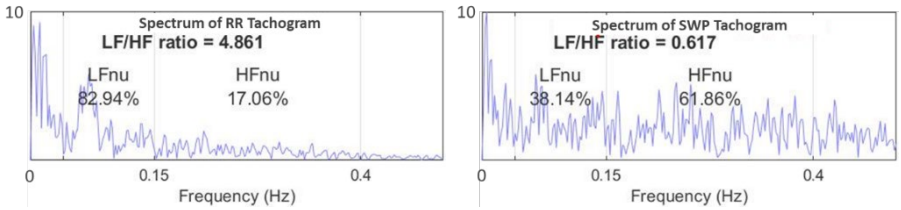

Figure II.24 *Subject 8: spectral analysis of the RR tachogram from ECG and SWP signals*

Chapter III
Sleepiness and Fatigue

III.1 Biology of human sleep and sleepiness

The terms sleepiness and fatigue (tiredness) are often indistinguishable when referring to a state of decay of the driver's condition: however they have different characteristics (Fig III.1). Somnolence is an intermediate state between wakefulness and sleep which has been defined as a state of progressive alteration of awareness associated with a physiological drive or inclination to sleep (Johns, 2000; Slater, 2008). Fatigue is considered one of the factors that can lead to sleepiness and it is a consequence of physical work or a prolonged experience: it is defined as a reluctance to continue the task (Brown, 1982). Some authors distinguish fatigue from sleepiness since the former does not fluctuate rapidly, for periods of a few seconds, such as sleepiness. Rest and inactivity usually relieve fatigue, however they make sleepiness worse (Johns, 2008).

Cognitively, studies have linked sleepiness and fatigue to decreased alertness (ability to detect and respond to unpredictable signals or events over a longer period of time), reaction time, memory, psychomotor coordination, information processing and decision making (Lyznicki, 1998; Isnainiyah, 2015). Its effects are stronger in those tasks which are monotonous, which have a long duration, which require constant attention and which have low predictability.

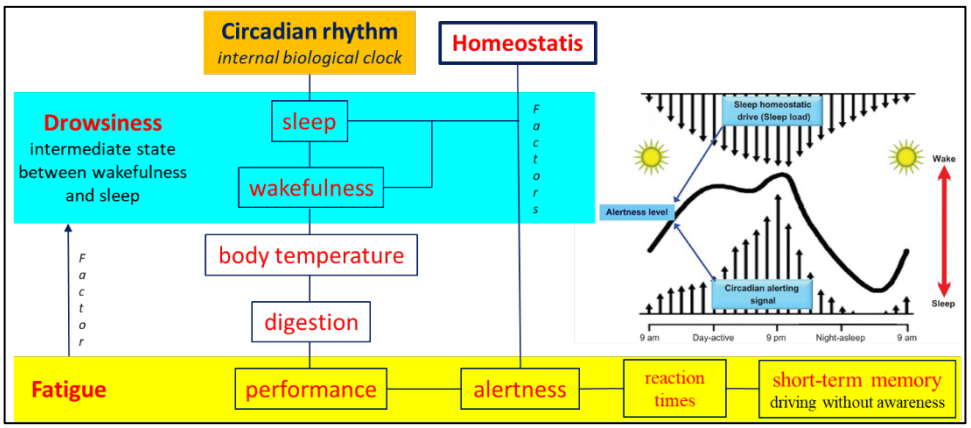

Figure III.1 *Effects of circadian and homeostatic factors on sleepiness and fatigue*

III.1.1 Performance impairment

In some activities, such as driving, sleepiness is considered a significant risk factor that contributes substantially to the increase in the number of car accidents each year (Campagne, 2004). Driver fatigue is believed to account for 35% -45% of all automobile accidents (Connor, 2009). About driving, there is a psychological conflict between the reluctance to drive and the need to drive. A result can be a progressive withdrawal of attention to the tasks required for safe driving (Treat, 1977).

Sleepiness leads to accidents because it alters elements of human performance that are critical to safe driving (Dinges, 1991). Relevant alterations identified in laboratory and vehicle studies include: slower reaction time (Dinges, 1995), reduced alertness (Haraldsson, 1990; Kribbs, 1994), information processing deficit (Dinges, 1995).

Many of these accidents are work-related, such as truck and commercial vehicle drivers. The effects of the time of day are profound, with sleepiness particularly noticeable during night work and after returning home. Circadian factors are as important in determining the driver's sleepiness as the duration of driving.

The circadian rhythm is an internal biological clock that completes a cycle approximately every 24 hours. It coordinates physiological priorities for daily activities, including sleep, body temperature, digestion, performance, and other variables. Therefore, it has a direct effect on alertness, mood, motivation and performance. Homeostatic factors govern circadian factors to regulate the times of sleepiness and wakefulness.

III.1.2 Causes and effects of drowsy driving

Although alcohol and some medications can independently induce sleepiness, the main causes of drowsiness while driving in people without sleep disorders are: sleep restriction or loss, sleep disruption and fragmentation, circadian factors.

Drowsiness accidents occur most often at night or in the mid-afternoon (off-peak hours), on motorways or state roads (driving more boring and at higher and steady speeds, involving only one vehicle and often with severe damage to the vehicle). The driver is usually alone and makes no effort to brake or take other actions to avoid the accident.

Car accidents are a leading cause of death worldwide and are expected to become the fourth leading cause of death in 2030 (WHO, 2011).

Sleepiness is the second leading cause (after alcohol) of car accidents. In numerous surveys, more than 50% of people report having driven drowsy during the last year, and almost 25% report having fallen asleep at the wheel (Horne , 1999; Sagaspe, 2010; Philip, 2014).

Some research has estimated that sleepiness plays a causal role, in whole or in part, in 20-25% of road accidents (WHO, 2011) and in about 20% of all fatal and serious accidents (Connor, 2002; Kecklund, 2011). In the case of truck accidents, tired and sleepy driving has been found to be a major cause (Chen, 2016) and 70% of these accidents are attributed to distraction (WHO, 2011).

The role of drowsiness, fatigue and driver tiredness and their impact on the incidence of road accidents are extensively documented in the literature (Connor, 2002; Bener, 2014; Herman, 2014; Williamson, 2014) and have been correlated with reduced performance in psychomotor tests and driving simulators (Lajunen, 2004; Herman, 2014; Thompson, 2014). Driver fatigue causes 1% -3% of road accidents and up to 20% of accidents occur on major roads and highways (Jamroz, 2013).

III.1.3 Evaluating sleepiness

A strategy to address this safety problem is to select the neurophysiological signals of motorists for the evaluation of mental workload, fatigue and sleepiness (Borghini, 2014), incorporating in the vehicle the driver status detection function in each moment by monitoring physical and driving performance (Daza, 2014).

Studies for the detection of sleepy and fatigued driving behavior have focused on two approaches: one adopts physiological signals, such as electroencephalogram (EEG) (Picot, 2012; Correa, 2014; Zhang, 2014; Li G., 2015) , heart rate variability (HRV) (Li G., 2013; Jung, 2014), time-averaged percentage of eye closure (PERCLOS) (Nagai, 2008; McDonald, 2012), facial features (Dikkers, 2004; Tianyi, 2010; Minjie, 2013) or the behavioral

characteristics (head position, sitting posture) (King, 1994; Wierwille, 1994a, 1994b, 1996; Sahayadhas, 2012) of the driver. The other approach adopts information on driving behavior and style, such as the position of the vehicle in the lane, the steering angles and the movements of the steering wheel. In turn, these methods are classified into intrusive and non-intrusive.

III.1.3.1 Vehicle-based tools

There are some onboard systems that are meant to measure sleepiness or certain behaviors associated with sleepiness. Examples include brainwave monitors, eye closure monitors, steering variance detecting devices, and lane deviation tracking devices (Dinges, 1995).

Fatigued drivers show changes in visual behaviors, i.e. in the way they move their eyes or blink. It has been shown that the frequency of blinking as well as vertical eye movement increases just before sleep (Hayami, 2002). Vitabile (2011) used the PERCLOS parameter to evaluate the performance of their designed system under real driving conditions.

The analysis of the driver's face image and the analysis of vehicle travel data are used to detect driver sleepiness (Mbouna, 2013; Cyganek, 2014). Driver's eye tracking is one of the most common methods of drowsiness detection applied in several studies (Picot, 2010; Lenskiy, 2012).

III.2 Fatigue

Fatigue is extreme tiredness, whether from physical or mental exertion or illness, caused by insufficient rest for a period of time. It is due to sleep loss and circadian misalignment and it is a serious threat to safety in occupations that require 24 hours of operation, irregular hours and extended working hours (Dawson, 1997; Van Dongen, 2003). Laboratory research has been instrumental in characterizing how changes in sleep duration and timing affect subsequent alertness and performance (Santhi, 2007).

III.2.1 Causes and effects of fatigue

Fatigue plays a negative role on quality of life and performance. Driver fatigue is an extended definition that includes drowsiness, reduced attention span and motivation to act, reduced alertness, changes in performance and a propensity to make mistakes.

On the other hand, fatigue can be seen as a signal from the body that the ongoing activity should be stopped, whether it is physical or mental activity or simply being awake. Although the causes of tiredness and drowsiness may be different, the effects of drowsiness and fatigue are very similar, namely a decrease in mental and physical performance.

Causes of fatigue:

- Lack of sleep or poor sleep: chronic or acute. Even the quality of sleep, influenced by sleep disorders, misalignment of the biological clock, noisy or unpleasant environment.
- Time-on-task: prolonged activity inevitably leads to physical and mental fatigue.
- Monotonous activity: driving for relatively long periods in a monotonous driving environment results in a decrease in the driver's alertness, which is an expression of fatigue.
- Individual characteristics: age, physical and medical condition, alcohol use also affect how quickly drivers get tired and how they manage to cope with it.

III.2.1.1 Effects of fatigue on driving

Research indicates that fatigue leads to deterioration in driving performance which results in less efficient information processing (reduced alertness, longer reaction times, reduced steering performance), lower short-term memory accuracy (e.g. example, a fatigued driver may not remember the previous few minutes of driving), poorer psychometric coordination and a greater tendency to mentally withdraw from the driving task (Brown, 1994; Dinges, 1995; Lyznicki, 1998; Philip, 2005). Drivers can use compensatory strategies to try to ward off the effects of fatigue. A phenomenon separated from fatigue, but often related to it, is "driving without awareness". Finally, it should be borne in mind that there are individual differences in how people react and cope with fatigue.

III.2.2 Evaluating fatigue

In the manifestations of fatigue, physiological and psychological components are distinguished. Fatigue is associated with physiological changes in brainwave activity, eye movement, head movement, muscle tone, and heart rate. With the onset of fatigue, body temperature, heart rate, blood pressure, respiratory rate and adrenaline production drop. A fatigued person can experience micro-sleeps. Micro-sleeps are short naps that last about four to five seconds.

Fatigue affects mood and motivation, as well as psychomotor and cognitive functions (Schagen, 2003). Fatigue is in part a subjective experience characterized by lack of motivation, feelings of exhaustion, boredom, discomfort, and a reluctance to continue a task. The psychological part of the fatigue has also been called "mental fatigue". Mental fatigue is a gradual and cumulative process and is associated with reluctance to commit, reduced efficiency and alertness, and impaired mental performance. A person's functional states range from deep sleep, light sleep, drowsiness, tired, barely awake, relaxed, restful, cool, alert, very alert, aroused, and an alert state. In

this series, mental fatigue is a functional state, which can result in sleep or a relaxed, restful condition (Lal, 2001).

III.2.2.1 Progression of fatigue

With the use of supervisory tasks, fatigue research has shown that periods of normal performance (i.e., seeing signals in time and providing the right response) alternate with short interruptions in operation (i.e., missing signals or responding very late). A theoretical explanation is that fatigue is not simply a passive process but is the result of an interaction between deactivation processes (e.g., slower functioning, less attention) and compensation processes. This means that a person can react when they notice the onset of fatigue and can compensate for the increased fatigue, for example, by engaging in more mental or physical effort to accomplish a task. The interaction between continuous fatigue and compensation (extra effort) leads to performance that becomes increasingly variable or unstable. Therefore, performance does not simply decline steadily, but with greater variability and even faster changes between normal operation and erratic operation (Dinges, 1991).

III.2.2.2 Vehicle-based tools

Fatigue warning systems have been proposed as specific countermeasures to reduce collisions associated with driver fatigue. These devices employ a variety of techniques to detect driver sleepiness while driving a vehicle and alert the driver when critical levels of sleepiness are reached. However, detecting driver fatigue using valid, non-intrusive and objective measures remains a significant challenge. Detection techniques can use lane departure, steering wheel activity, eye or facial features. Several authors point out that fatigue warning systems can provoke a behavioral adaptation of the driver (Sagberg, 1999). A possible negative effect of on-board warning systems could be that the driver uses them to stay awake and drive for longer periods instead of stopping and taking a nap: thus, compensating for risk by relying too much on the safety system.

A system that uses multiple components (for example, operator and performance monitoring) is probably more effective than one that focuses on just one dimension. Each system has advantages and disadvantages. An important consideration in the implementation of these systems, which so far has not been adequately addressed, is the acceptance and use of the system by road users (Horrey, 2011; Salvati, 2020).

Recent technological developments in the field of fatigue detection include the use of artificial vision to detect driver drowsiness (Chakraborty, 2014; Massala, 2014) and the use of non-intrusive biopotential measurement systems that do not require contact with the human skin (Sun, 2014).

III.3 HRV for sleepiness and fatigue recognition

Changes associated with sleep phase transitions affect the autonomic nervous system (ANS) and cardiac activities (Trinder, 2001; Versace, 2003) and HRV can be used as an indicator of the ANS responses to stress, sleepiness and other factors related (Malik, 1996; Jurysta, 2003; Li, 2013; Tobaldini, 2013), as well as to identify the lack of attention. Several previous studies have concluded that heart rate (HR) varies significantly between alertness and sleepiness state (Liang, 2009; Miyaji, 2009) and that HRV-based methods are able to recognize driver sleepiness (Jiao, 2004; Shin, 2010; Yang, 2010; Patel, 2011; Mahachandra, 2012).

Chui (2016) proposed a method of detecting sleepiness based on an electrocardiogram (ECG) taken from drivers. Additionally, some researchers analyzed photoplethysmography (PPG) signals to detect sleepy driving (Lee, 2011). Although they reported that the proposed methods were capable of achieving good performance, it is difficult to obtain good ECG or PPG signals stably due to motion artifacts. Furthermore, these methods would require a heavy computational load because the ECG sampling rate is usually greater than several hundred Hz.

There is a strong relationship between the LF/HF ratio and the driver's fatigue level (Patel, 2011), although the results for the LF/HF ratio are less consistent. Some research (Jiao, 2004; Shin, 2010; Mahachandra, 2012) has concluded that the LF/HF ratio increases when driver drowsiness occurs, while others (Yang, 2010; Patel, 2011) have found that the LF/HF ratio it progressively decreases as the driver goes from an alert state to a drowsy state.

Chapter IV
On-road Test

IV.1 On-road detection of driver fatigue and drowsiness on medium-distance journeys

The following study presents a road driving experiment with non-intrusive instrumentation, with a triple goal: (a) to collect a database of physiological signals from both wakeful and drowsy drivers, useful for studying the measurable changes related to falling attention and fatigue/sleepiness; (b) to define a continuous control index based on the long-term cardiac signal variation and compare it with the PERCLOS indicator for the classification of the sleepiness phases; (c) to identify patterns for the recognition of ANS activation and prevalence phases that allow us to distinguish the different phases of sleepiness and prevent it.

PERCLOS70 or PERCLOS80 (percentage of time the eyes are closed for more than 70 or 80%) is the most reliable parameter in detecting sleepiness (Dinges, 1998; Bhuiyan, 2009).

IV.1.1 Materials and Methods

This section describes the sleepiness detection procedure based on heart rate variability (HRV) acquired through a sensor integrated in the seat back that allows constant contact with the driver's body (Murata, 2011). The characteristics of the cardiac signal are extracted from the RRI data (interval between wave peaks) recorded while driving and the information obtained from the analysis of this signal is used in a predictive algorithm that provides the closest sleepiness/fatigue index possible to the values obtained with the PERCLOS indicator and which also manages to highlight a trend of sleepiness/fatigue phases (Sagberg, 2004). In turn, the levels of sleepiness and fatigue are quantified using the Karolinska Sleepiness Scale (KSS) and the driver's subjective estimate, respectively.

We used a universal model for the detection of sleepiness that did not take into account the individuality of the driver and that was able to provide a real-

time assessment free from the need to previously acquire an identification model of sleep and wakefulness states for comparative purposes.

IV.1.1.1 Detection system

The information relating to the heartbeat is obtained through the analysis of the acoustic pulse wave: this signal is recorded through a capacitive microphone sensor embedded in a specific support made of 3D polyester material and inserted into the seat cover. This material acts as an oscillator with a centre frequency of approximately 20 Hz and, through the phenomenon of stochastic resonance, allows both the filtering of the acoustic signal around 20 Hz for the removal of artifacts and the maximum coupling of mechanical impedance between the subject's trunk and the sensor. This technique allows to reduce to a minimum the number of undetected beats with consequent improvement of the reliability of the analysis (Hagiyama, 2018, 2019).

IV.1.1.2 Analytical model

The cardiac signal is filtered to eliminate the noise components due to respiration or movement artifacts: the information on the vibration due to the heartbeat is contained in signals around 20 Hz (Hagiyama, 2018, 2019) which are therefore passband filtered from 10 to 30 Hz. In order for this signal to take on the waveform of the cardiac cycle (having a frequency close to 1 Hz), it is further passband filtered between 0.8 and 2.0 Hz (Figure IV.1). A second-order Butterworth IIR bandpass filter is applied.

The waveform thus obtained (Figure IV.2) allows us to evaluate two types of interval: the one between the peaks and the variability of which in terms of average frequency detected in constant time segments we believe is useful for identifying the prevalence states of the Parasympathetic Nervous System (PSNS) and therefore any conditions of exhaustion; and the interval between the points of intersection with the zero baseline whose spectral analysis is used to estimate a decrease in sympathetic nervous activity (SNS), i.e. a reduced level of arousal linked to the occurrence of drowsiness episodes (Baharav , 1995; Furman, 2008; Shin, 2010).

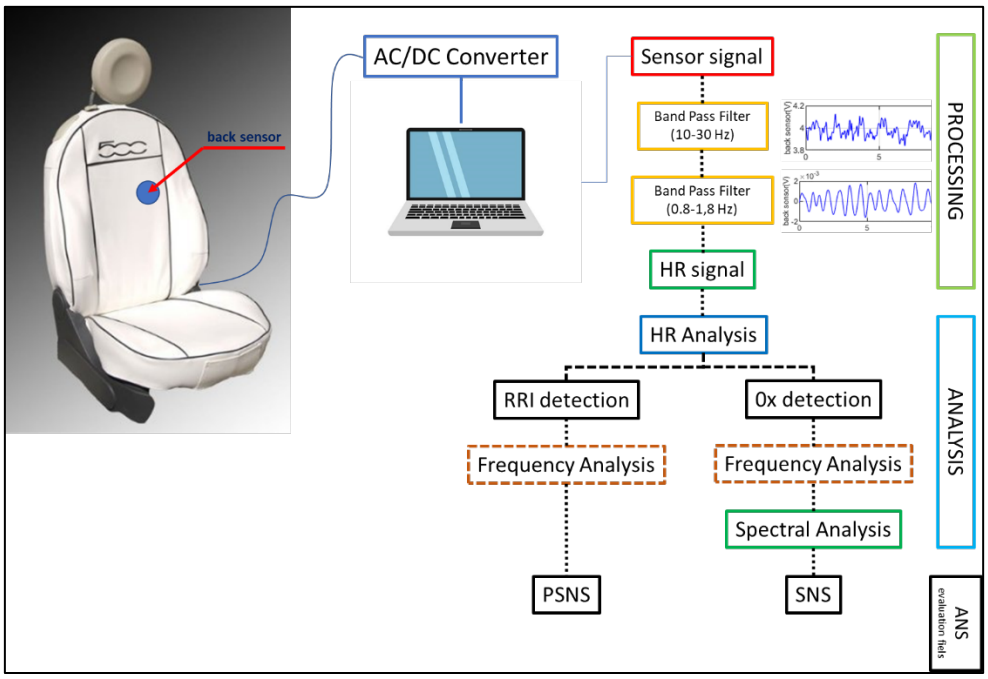

Figure IV.1 *Signal processing*

The intervals between peaks and between zero-line crossing points are first converted into the corresponding frequencies and these ones, in turn, are averaged over a 5-second interval (Figure IV.3). This technique allows to produce an output even if the sensor fails to pick up the cardiac signal.

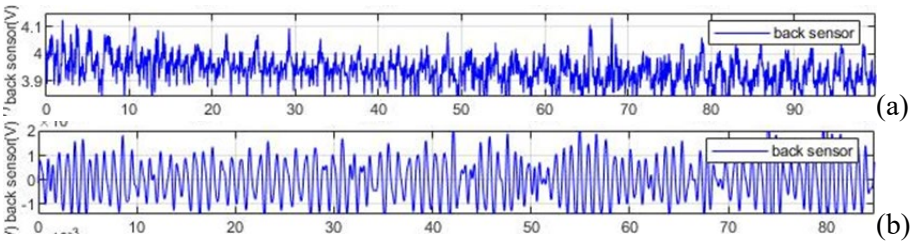

Figure IV.2 *Heartbeat signal: before (a) and after (b) processing*

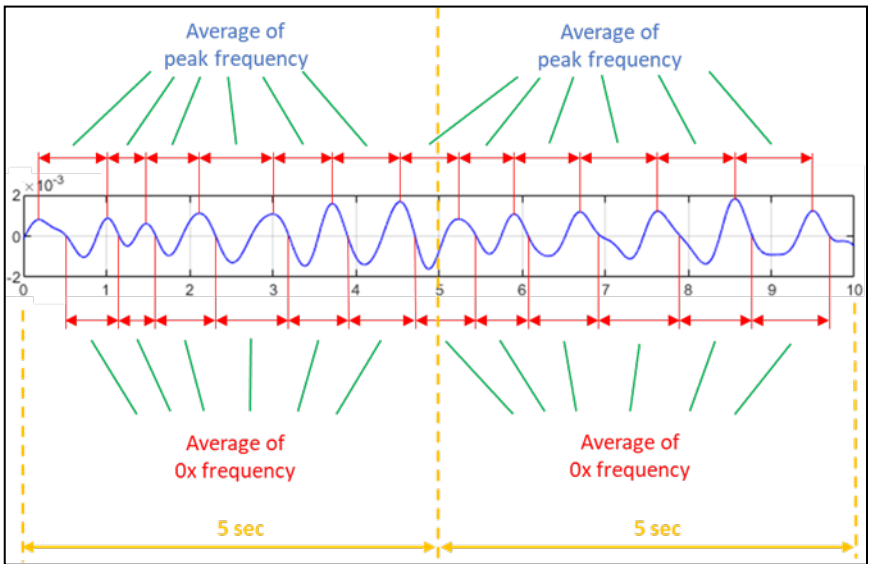

Figure IV.3 *Calculation of the average frequency*

This average frequency is shown on the ordinate of the graph in Figure IV.4: a sequence of 5-second spaced points is thus formed. On a 180-second time window, the linear regression line is identified (least squares method); then you move on the abscissa axis 18 seconds at a time, calculating each time the new linear regression line. This procedure applies to both peaks and 0x points.

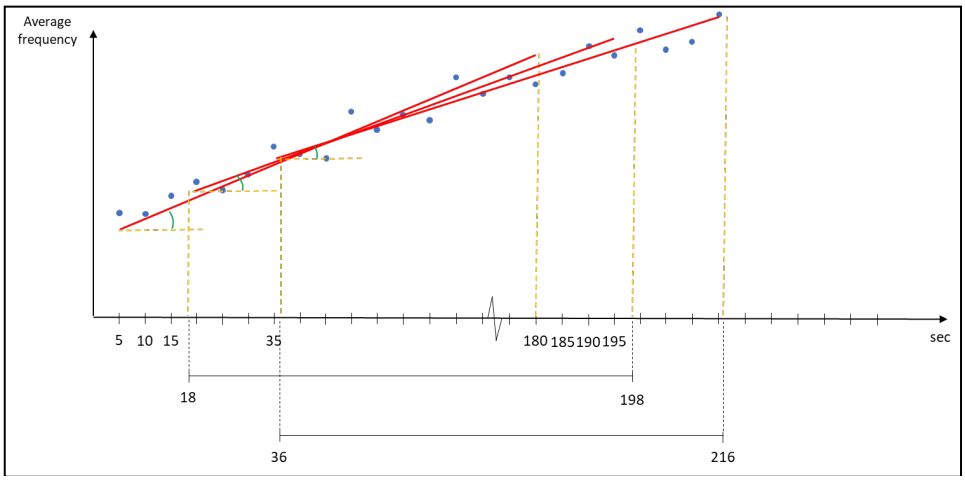

Figure IV.4 *Identification of linear regression lines on moving time windows*

The arithmetic mean of the points in the 180-second window allows to draw the first graph of Figure IV.5 (Average of Freq), interpolated as the points are obtained every 18 seconds. The inclination of the regression lines determines the value of the ordinates on the interpolated graph of the Frequency Gradient (second graph of Figure IV.5).

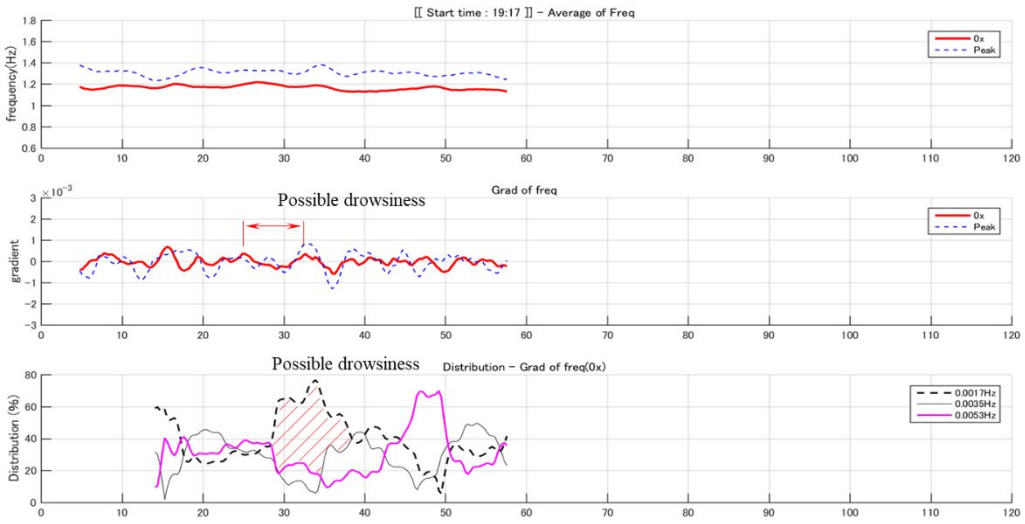

Figure IV.5 *Processing of trends: average of frequency, gradient of frequency and spectral distribution*

In the frequency gradient graph, it was observed that with an elongation of the interval between the peaks of the 0x wave, predictive signs of sleepiness appear; it becomes imminent sleep when the waveform converges until it flattens out. Furthermore, when the amplitude of the wave increases it indicates the onset of a hypnagogic state (which is the consciousness state of transition from wakefulness to sleep), while when it decreases it indicates the transition from a state of opposition to sleep to that one of partial recovery.

In order to determine the fatigue state, it is necessary to evaluate the changes in the human condition in long-term cycles that can be highlighted by analyzing the ultra-low frequency components of HRV (Serrador, 1999). Similarly, human homeostasis manifests itself through fluctuations in an ultra-low frequency band ULF (Figure IV.6): the region between 0.001 and 0.007 Hz is believed to contain information relating to long-term regulation (Fujita, 2005; Ochiai, 2006), in particular there are fluctuations in the frequency band around 0.0017 Hz (whose signal is associated with a decrease in sympathetic activity), 0.0035 Hz (associated with the evolution of the fatigue level) and 0.0053 (it expresses the level of control exerted by the SNS during an activity).

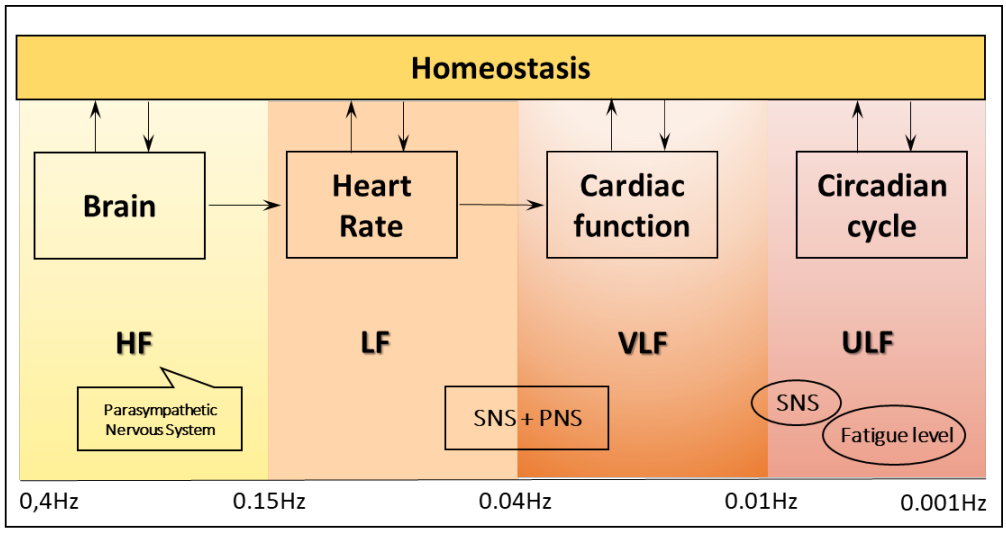

Figure IV.6 *Homeostatic control system*

The third graph of Figure IV.5 is the spectral distribution resulting from the application of the FFT to the frequency gradient of the 0x points, taking into consideration only the components with a frequency between 0-0.0017 Hz, 0.0017-0.0035 Hz, 0.0035 -0.0053 Hz.

From the analysis of the frequency trend of the intersection points with the zero line, assuming 100 the total values of the power spectra of the aforementioned frequency components, a spectral distribution with three waveforms is obtained (third graph in Figure IV.5). Taking into consideration the results relating to the tests in which episodes of drowsiness occurred, by examining the graphs of the percentage distribution frequency, it is observed that in the imminence of the periods in which drowsiness or falling asleep is reported occurs the condition:

$$\frac{\theta+\alpha}{\beta} > 2 \qquad \theta, \alpha > \beta \qquad \text{(IV.1)}$$

and more precisely it is possible to associate the sleep state to the case in which $\theta > \alpha$ and the drowsiness state to the case in which $\alpha > \theta$. In the case $\alpha \gg \theta$, with ascending α and θ steady, it can be assumed that there is fatigue of the subject. The increase in the distribution of α (ascending) compared to θ (descending) can mean that the organism tries to resist sleep, while the increase in β can indicate the resumption of an activation state because, in cases where no onset of drowsiness occurred, this distribution has concentrated peaks in the 20-60% range, while in cases where drowsiness occurred this distribution had concentrated peaks in the 0-30% range (Salvati, 2021).

IV.1.1.3 Drowsiness Scale

KSS is a self-signaling method in which the driver is asked every 15 minutes to provide a number between 1 and 9 of their sleepiness level (1 indicates fully aware and 9 indicates a very sleepy condition). However, this method has two limitations: it is unable to continuously monitor the driver's sleepiness and it is based on self-assessment, while based on our experiments drivers often do not have a precise idea of their level of sleepiness. To reduce this negative effect, a camera was installed on the car's dashboard in order to capture the driver's face during his performance and to be able to evaluate the PERCLOS index.

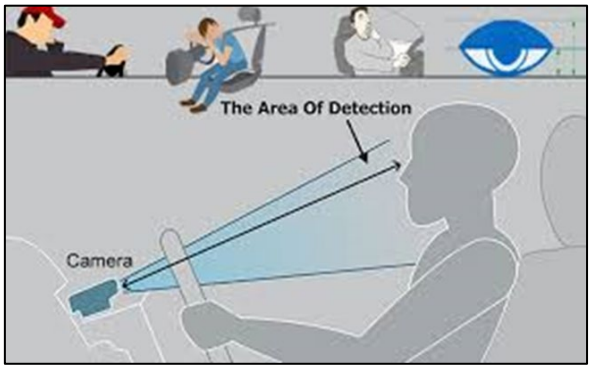

Fig IV.7 *Positioning of the camera*

In calculating this parameter, we took into account any manifestation of drowsiness (70% of partial closing of the eyelids, blinking, yawning). The detection was divided into "i" frames of 10 seconds, giving each of them the value 1 in the event of drowsiness and the value 0 in the opposite case. The PERCLOS index was evaluated every minute as an average of 6 frames:

$$\text{PERCLOS} = \frac{\sum_{i=1}^{6} Drowsiness\ event\ [i]}{6} \times 100\ (\%) \qquad \text{(IV.2)}$$

where by “Drowsiness event” we mean the occurrence of any of the three manifestation of drowsiness aforementioned.

In this way, 6 ranges of values were identified (0-0.33, 0.34-066, 0.67-1), grouped two by two so as to distinguish three different macro-areas: alertness, hypovigilance and sleepiness. To take into account the effect of fatigue on the conditions of sleepiness and the weight of the subjective judgment which corresponded to a more or less high level of fatigue at each level of sleepiness, a scale was also defined for the algorithm used with values 0 to 12 that could adjust to the levels of sleepiness and fatigue expressed with the KSS (Table IV.1).

Table IV.1 *Drowsiness level description*

Karolinska Sleepiness Scale			Post-Processed Sleepiness Scale	
Level	**Verbal description**	**Vigilance stage**	**Level**	**Verbal description**
1	extremely alert	alertness	0	
2	very alert		1 2	negligible signs of fatigue
3	alert		3 4	
4	rather alert	hypovigilance	5	
5	neither alert nor sleepy		6	slight fatigue
6	some signs of sleepiness		7 8	
7	sleepy, but no effort to keep alert	drowsiness	9	increasing fatigue and drowsiness
8	sleepy, some effort to keep alert		10 11	slight drowsiness
9	extremely sleepy, fighting sleep		12	strong drowsiness

IV.1.1.4 Experimental Protocol

IV.1.1.4.1 Experiment Environment

The tests were carried out on a motorway circuit 46.2 km long (Figure IV.8), which was run twice in the afternoon to allow for smooth traffic conditions. The total time taken is approximately 1h 35m. The speed limit was imposed at 80km/h. The car used is a city car without driver assistance systems and equipped with a seat cover containing the microsensor for detecting the heart signal.

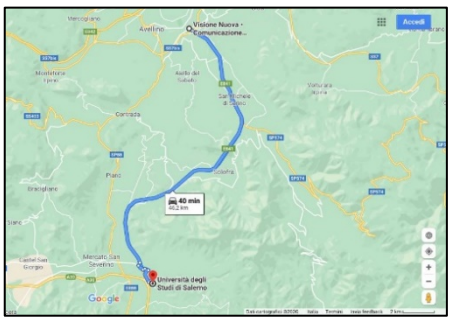

Figure IV.8 *Test course*

IV.1.1.4.2 Experiment Subjects

Three drivers over the age of 30 performed this experiment for a total of 14 sessions. They are healthy males with decades of driving experience. FCA professional drivers were recruited and test were performed during routine workday's activities, with all participants that received an explanation about the purpose of test and signed their informed consent. The subjects were asked to sleep at least 7 hours the night before the driving experiment, not to smoke and not to take caffeine, alcohol or energy drinks after waking up until the time of the experiment. This preparation allows to replicate in a more realistic way natural conditions of fatigue and postprandial sleepiness. Before starting the test, each driver adjusted the backrest so that his back was naturally in contact with the seat: this action allowed for constant body contact with the seat cover.

IV.1.1.4.3 Data Acquisition

Driving information is collected on the car in real-time, including the heart signal at a sampling rate of 200 Hz and the video recording of the driver's face, who is also administered a self-assessment questionnaire of their drowsiness and fatigue. The videos with the driver's oral assessment every 15 minutes help to estimate the driving status and create a corresponding set of learning data useful for defining the level scale used as the output of the algorithm.

IV.1.1.4.4 Experimental Procedure

The driving experiment consisted in completing the path outlined twice without stopping so that the conditions of the participants were monitored for at least an hour and a half and they could be in a more realistic state of sleepy/fatigued driving. Drivers reported their feelings on the degree of sleepiness/fatigue every 15 minutes according to the KSS scale.

IV.1.2 Results

The data relating to the individual experiments were evaluated independently and not aggregated by subject or time of execution, so as to be able to analyze the performance in an absolutely random manner and obtain an analysis independent of the subjectivity of each driver's conditions (health, emotional, sleep, fatigue). Since the PERCLOS index is calculated every minute while that of the algorithm provides a result every 18 seconds, it was decided to evaluate the correspondence of the levels to which the numerical indices belong every 5 minutes for a total of 275 detections distributed in the 14 tests performed.

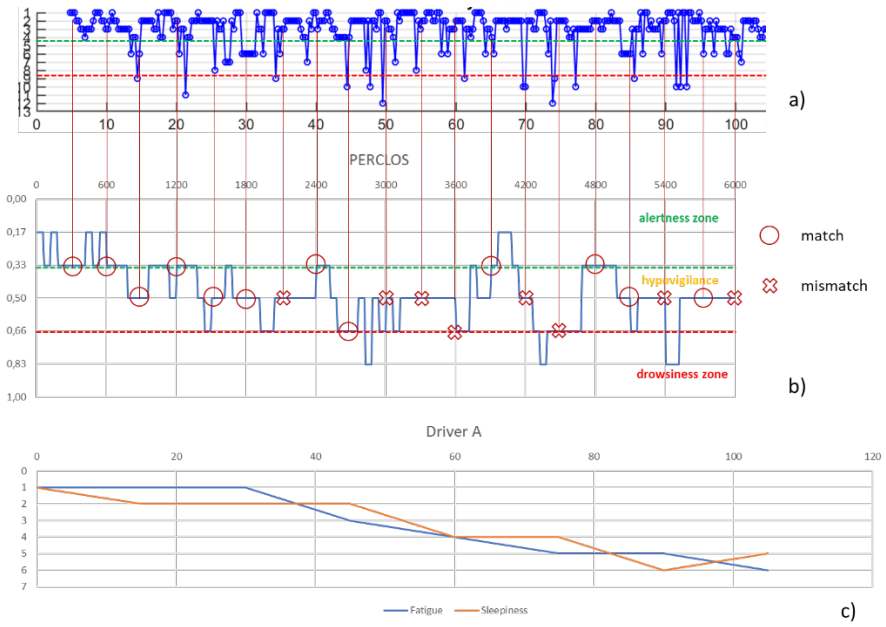

Figure IV.9 *Driver A's detections: a) algorithm score, b) PERCLOS index, c) subjective evaluation*

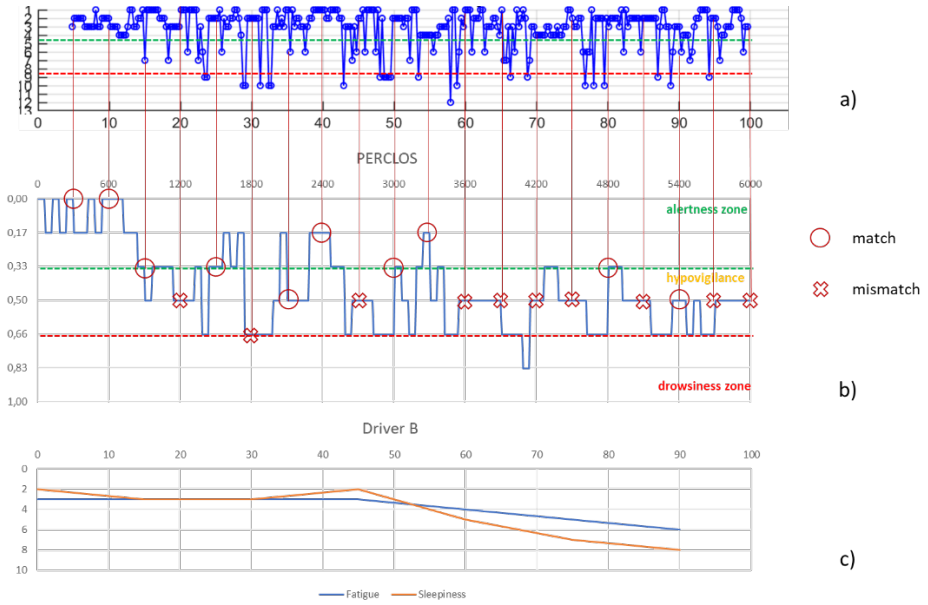

Figure IV.10 *Driver B's detections: a) algorithm score, b) PERCLOS index, c) subjective evaluation*

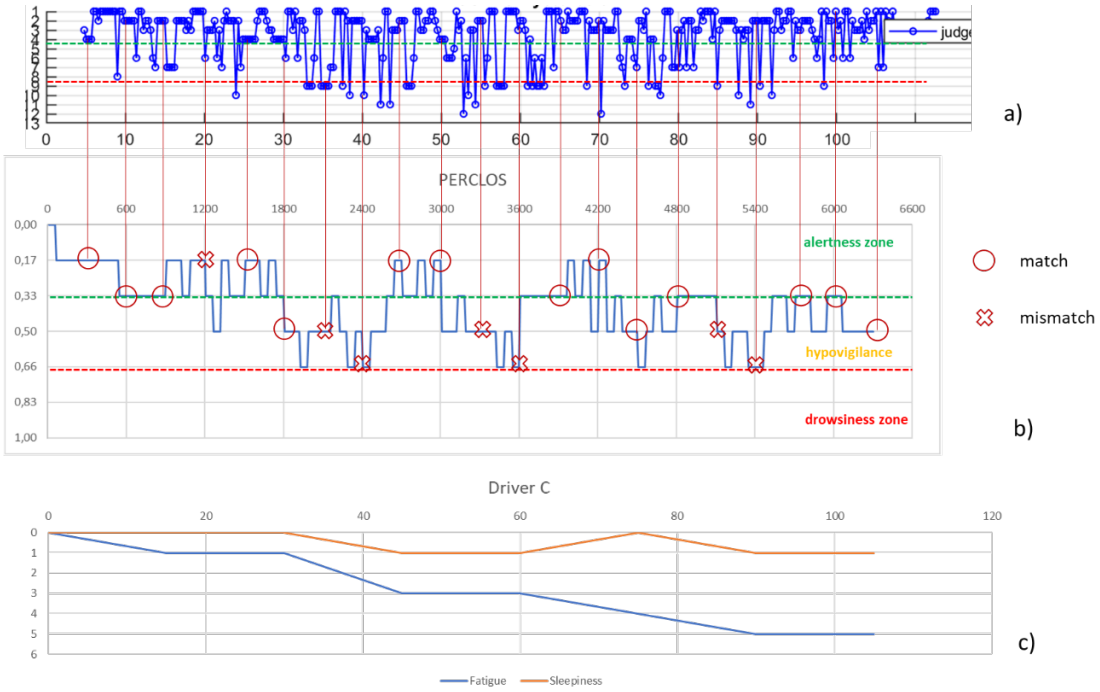

Figure IV.11 *Driver C's detections: a) algorithm score, b) PERCLOS index, c) subjective evaluation*

For explanatory purposes, Figures IV. 9-10-11 show the cases relating to three of the participating subjects: in a) the graph of the values resulting from the algorithm used for the assessment of sleepiness, in b) the PERCLOS index and in c) the driver's subjective assessment are shown. In each graph, the three macro-areas that had been defined in the sleepiness scale were distinguished and to evaluate the accuracy of the algorithm it was considered that there was a correspondence of the result in the case in which the values of the PERCLOS and of the index calculated with the algorithm fell into the same macro-area. Therefore, the accuracy thus calculated is 63%. The predictive effectiveness of the algorithm was also assessed by considering, in correspondence with each of the 275 detection events, the trend of the scores arising in the 5 minutes or 90 seconds prior to the evaluation of PERCLOS: respectively 16 and 5 scores were considered and the macro-area was attributed to the trend according to where the relative majority of its points fall. The accuracy was respectively 44% and 56% (Table IV.2) highlighting that, given the considerable variability in the measurement of the trend of fatigue and related sleepiness, the algorithm is less efficient when a history of previous values is incorporated, but more accurate when taking into account values closest to the chosen detection point.

Table IV.2 *Accuracy indices*

Driver	test	n° of detections	match	matching with the last 5-min trend of scores	matching with the last 90-sec trend of scores
A	1	19	13	9	12
	2	18	11	7	11
	3	20	12	9	9
	4	21	14	10	12
	5	20	12	8	13
B	1	18	12	9	10
	2	19	13	9	12
	3	18	12	7	12
	4	18	12	8	10
	5	19	10	6	7
C	1	22	13	9	10
	2	22	12	8	8
	3	21	14	9	11
	4	20	12	7	9
tot	14	275	172	115	146
Success %			63	44	56

Comparing the self-assessment graphs of sleepiness/fatigue with the PERCLOS index it is evident that, on the one hand, the driver's state does not necessarily reflect in expressive or behavioral manifestations typical of a stressed condition, on the other hand the driver does not have a clear perception of his state enough to be able to quantify it. However, the subject's judgment was useful in defining a drowsiness scale in which the effect of fatigue could be taken into account.

From the comparison of PERCLOS with the results of the used model, it is observed how the evaluation of the driver's status shows similar trends, although failing to ensure high accuracy at all times, especially in the transition phases which turn out to be the cause of error in 82% of cases.

The drowsiness detection model described is sufficiently adherent to the state of the monitored drivers, at least as long as they are not in limit conditions. The difficulty of carrying out tests on real vehicles to detect the conditions of the driver in a state of sleep deprivation is one of the main limitations to experimentation.

In this study, the potential of an algorithm for identifying the driver's sleepiness/fatigue states was evaluated. This was achieved by analyzing the corresponding physiological signals, from the eyes and the heart.

The obtained results have not currently exceeded the accuracy of feature extraction methods based on the detection of blinking, facial expressions or steering angle. However, this system overcomes some of the limitations of these techniques as it allows continuous and contactless monitoring, limits interference related to environmental factors (brightness, bumpy paths) or contingent ones (use of glasses, head movements) and makes use of devices without contraindications.

Being able to perform tests of longer duration and in more critical conditions for the subjects would allow us to know how the physiological conditions change in the state of transition from wakefulness to sleep and how the subject manifests his opposition to physical failure.

Chapter V
Further Developments

V.1 New possibilities for use

The possibility of equipping a seat with two sensors, one in the backrest and the other on the seat (Figure V.1), offers the opportunity for further development of the model developed: always with a view to daily monitoring of the subject/driver's conditions, the idea of arriving at the measurement of pulse wave velocity (PWV) appears feasible. It is generated by the ventricular ejection and represents the speed with which the arterial impulse propagates in the cardiovascular system with a speed determined by the geometric and elastic properties of the arterial wall. This parameter increases with age and it has a strong correlation with cardiovascular diseases and mortality and it has been recognized by the European Society of Hypertension as an indicator of arterial stiffness, as well as a test for the search for hypertension: the more its value the higher, the greater the arterial stiffness. A high pulse wave speed has also been associated with reduced lung function (Townsend, 2015).

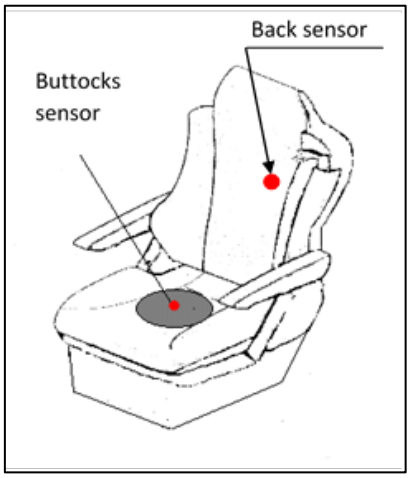

Figure V.1 *Seat equipped with double sensor*

By definition, PWV is the distance traveled by the wave, divided by the time thewave takes to travel that distance: $PWV = \Delta x/\Delta t$. This is true for a system with zero reflected waves. The transmission of the blood pressure pulse does not give the true PWV, as this is the resultant of the incident wave vectors and the reflected waves ones (Figure V.2).

To calculate the PWV it is necessary to detect the pressure wave through a tonometric sensor positioned at the level of two different arterial pulses or with techniques such as ultrasound or Doppler to monitor the flow.

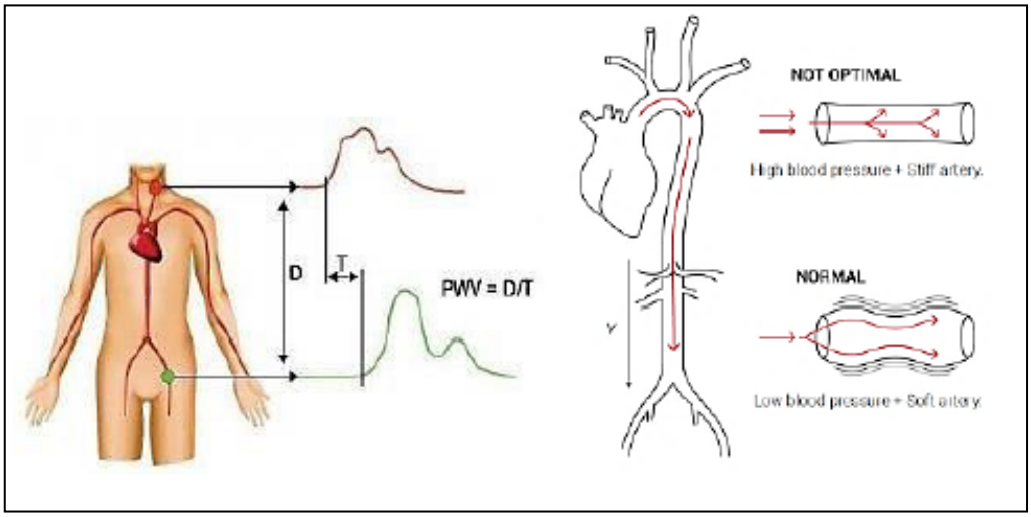

Figure V.2 *Aortic PWV is defined as the average velocity of a pressure pulse when travelling from the aortic valve, through the aortic arc until it reaches the iliac bifurcation*

At the moment, although this type of survey has been carried out, some considerations remain to be answered:

- it is necessary to validate the PWV measurements with clinical instrumentation applied to the subject when he is seated;
- the sensors are unable to detect the incidence of the reflected wave of the sphygmic pulse: a problem that could affect the results.

As it can be seen from a generic survey performed on two of the subjects involved in the previous tests, the reflected wave is very marked in the acquisitions with photoplethysmograph (PPG) compared to that obtained with the sensors placed in the backrest or on the seat (Figura V.3).

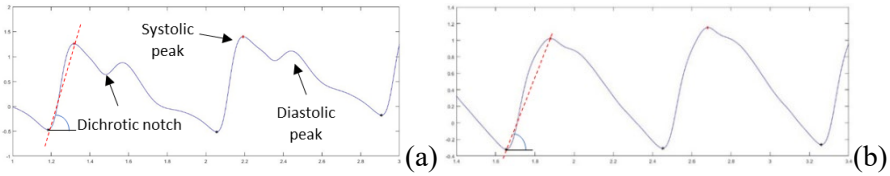

Figura V.3 *PPG signal for (a) Subject 1 (25 y.o.), (b) Subject 5 (54 y.o)*

Conclusions

The research project was born from the collaboration of two groups engaged in the automotive sector, FCA Group and Delta Kogyo (manufacturer of car seats), with the aim of developing reliable tools for the investigation of tiredness or drowsiness at the wheel, exploring a road still today little traveled except from a clinical point of view: the processing of the cardiac signal for the identification of the driver's status, moreover from the point of view of a skin-contactless system, undoubtedly represents an innovative challenge in the market of car manufacturers.

The path that led to the definition of a device that meets these specifications began with the search for a pseudo-ECG signal detection system that did not provide for direct contact with the individual's skin. In the next phase, in order to limit the margins of error due to signal noise and to ensure that these inconsistencies with the actual ECG signal were not reflected in the output of the algorithm, it was developed a method that modeled the variations of the signal on a mobile window of time that is wide enough to be able to level any anomalies and allow to evaluate changes in the driver's status more effectively.

The assessment of driver fatigue involved the measurement of biomedical signals, environmental data and the analysis of eyelid activity (based on the analysis of the images acquired by the on-board camera). The metering devices, their architecture and the communication method were also described. The study described the non-contact measurement of the ECG signal with the use of a sensor installed in the driver's backrest, under the seat upholstery. As a result, the driver does not feel the sensors, which therefore does not cause any discomfort while driving. The sensor signal is much weaker (about ±5 mV) than the signal received by the electrodes applied to the subject's body (about ±0.5 V). However, it allows you to determine the signal of the heart's electrical activity.

Eyelid movement research allows real-time determination of the PERCLOS parameter, supporting the process of identifying the driver's fatigue level.

It is possible to process the signal both online and offline, therefore this model can be the basis for the development of an objective method of

measuring the risk that occurs while driving, resulting from changes in the psychological and physiological conditions of the driver.

The experiments that were described in the last study were carried out on the road, on medium-range routes and in the afternoon and, for safety reasons, it was avoided that the drivers were in exhausting conditions, extremely tired or sleepy. Therefore this setting produced short periods of inattention, but the result obtained could actually reflect a more realistic situation, since a driver cannot remain asleep for more than a few seconds without having an accident (Reyner, 1998) and the typical risk of accident due to fatigue does not occur in a deep and prolonged state of drowsiness, but of "microsleep" or a transient drop in attention in critical maneuvers.

Bibliography

Akerstedt T., Peters B., Anund A. and Kecklund, G. (2005) Impaired alertness and performance driving home from the night shift: a driving simulator study. *Journal of Sleep Research*, 14(1), 17–20.

Akselrod S. Components of heart rate variability: basic studies. *In:* Malik M., Camm A.J., editors. *Heart rate variability*, 1995 Armonk, N.Y.: Futura Publ. Comp., Inc., 147–63.

Avolio A.P., Van Bortel L.M., Boutouyrie P. (2009) Role of pulse pressure amplification in arterial hypertension: experts' opinion and review of the data. *Hypertension*, 54, 375-383.

Baharav A., Kotagal S., Gibbons V., Rubin B.K., Pratt G., Karin J., Akselrod S. (1995) Fluctuations in autonomic nervous activity during sleep displayed by power spectrum analysis of heart rate variability. *Neurology*, 45(6), 1183–1187.

Bener A., Razzak J.A., Crundall D. (2014) The relationship between four-wheel drives and risky driving behaviours: lesson learning from traffics crashes in Qatar. *International Journal of Medicine and Public Health*, 4(3), 280-286.

Bhuiyan M.S. (2009) Driver assistance systems to rate drowsiness: A preliminary study. *New Adv. Intell. Decis. Technol.*, 199, 415–425.

Bompiani (1990) Circolatòrio, apparato. *In:* Etas S.p.a., *Enciclopedia Bompiani*. Milano: 213-218.

Borghini G., Astolfi L., Vecchiato G., Mattia D., Babiloni F. (2014) Measuring neurophysiological signals in aircraft pilots and car drivers for the assessment of mental workload, fatigue and drowsiness. *Neurosci. Biobehav. Rev.*, 44, 58–75.

Bos J.E., Bles W. and Groen E.L. (2008) A theory on visually induced motion sickness. *Displays*, 29 (2), 47–57.

Bramwell J.C., Hill A.V. (1922) The velocity of the pulse wave in man. *Proc R Soc Lond (Biol)*, 93, 298-306.

Brennan M., Palaniswami M., Kamen P. (2001) Do existing measures of Poincare plot geometry reflect nonlinear features of heart rate variability? *IEEE Trans. Biomed. Eng.*, 48, 1342–1347.

Brown I. D. (1982) Driving fatigue. *Endeavour*, 6(2), 83–90.

Brown I. D. (1994) Driver Fatigue. Hum Factors, 36(2), 298-314.
Campagne A., Pebayle T. and Muzet A. (2004) Correlation between driving errors and vigilance level: Influence of the driver's age. *Physiol. Behav.*, 80(4), 515–524.
Cerutti S., Bianchi A.M., Mainardi L.T. (1995) Spectral analysis of the heart rate varibility signal. *In:* Malik M., Camm A.J., editors. *Heart rate variability*, 1995, Armonk, N.Y.: Futura Publ. Comp., Inc., 63–74.
Chakraborty M. and Hossain A.N. (2014) Implementation of Computer Vision to Detect Driver Fatigue or Drowsiness to Reduce the Chances of Vehicle Accident. *International Conference on Electrical Engineering and Information & Communication Technology* (ICEEICT), 1-5.
Chen G. X., Fang Y., Guo F. and Hanowski R. J. (2016) The influence of daily sleep patterns of commercial truck drivers on driving performance. *Accident Analysis & Prevention*, 91, 55–63.
Chui K. T., Tsang K., Chi H. R., Ling B., Wu C. (2016) An accurate ECG-based transportation safety drowsiness detection scheme. *IEEE Trans. Ind. Inform.*, 12(4), 1438–1452.
Clifford G.D. (2005) Quantifying errors in spectral estimates of HRV due to beat replacement and resampling. *IEEE Trans. Biomed. Eng.*, 52, 630–638.
Connor J., Norton R., Ameratunga S., Robinson E., Civil I., Dunn R., Jackson, R. (2002) Driver sleepiness and risk of serious injury to car occupants: Population based case control study. *British Medical Journal*, 324, 1125-1128.
Connor J.L. (2009) The role of driver sleepiness in car crashes: A review of the epidemiological evidence. In: Springer *Drugs, Driving and Traffic Safety*. Basel, Switzerland: 187–205.
Correa A.G., Orosco L., Laciar E. (2014) Automatic detection of drowsiness in EEG records based on multimodal analysis. *Med. Eng. Phys.*, 36, 244–249.
Cyganek B. and Gruszczynski S. (2014) Hybrid computer vision system for drivers' eye recognition and fatigue monitoring. *Neurocomputing*, 126(27), pp. 78–94.
Dawson D., Reid (1997) K. Fatigue, alcohol and performance impairment. *Nature*, 388(6639), 235.
Daza I.G., Bergasa L.M., Bronte S., Yebes J.J., Almazán J., Arroyo R. (2014) Fusion of optimized indicators from Advanced Driver Assistance Systems (ADAS) for driver drowsiness detection. *Sensors*, 14, 1106–1131.
Dikkers H.J., Spaans M.A., Datcu D., Novak M. and Rothkrantz L.J.M. (2004) Facial Recognition System for Driver Vigilance Monitoring. *IEEE International Conference on Systems, Man and Cybernetics (IEEE Cat. No.04CH37583)*, The Hague, Netherlands, 4, 3787-3792.

Dinges D. F. and Kribbs N. B. (1991) Performing while sleepy: effects of experimentally induced sleepiness. *In:* Monk, T. H. (Ed.) *Sleep, Sleepiness and Performance*. Wiley, Chicester: 97-128.

Dinges, D. F. (1995) An overview of sleepiness and accidents. *Journal of Sleep Research*, 4(2), 4-14.

Dinges, D. (1998) PERCLOS: A valid psychophysiological measure of alertness as assessed by psychomotor vigilance. *In:* Tech. Rep. MCRT-98-006, Federal Highway Administration, Office of motor carriers.

European Commission (2015) *Driver distraction*. European Commission, Directorate General for Transport.

Faber, J. (2004) Detection of different levels of vigilance by EEG pseudo spectra. *Neural Network World*, 14 (3-4), 285–290.

Fujita E., Ogura Y., Ochiai N., Miao T., Shimizu T., Kamei T., Murata K., Ueno Y., Kaneko S. (2005) Development of the measurement method of the prediction of sleep by finger plethysmogram data. *The Japanese Journal of Ergonomics*, 41(4), 203-212.

Furman G., Baharav A., Cahan C., Akselrod S. (2008) Early detection of falling asleep at the wheel: a heart rate variability approach. *Comput Cardiol*, 1109–112.

Golińska K. A. (2013) Poincaré Plots in Analysis of Selected Biomedical Signals. *Stud. Log. Gramm. Rhetor.*, 35, 117–127.

Hagiyama N., Mito A., Hirano H. (2018) Unconstrained Monitoring of Biological Signals Using an Aortic Pulse Wave Sensor. 40th Annual International Conference of the IEEE Engineering in Medicine and Biology Society (EMBC).

Hagiyama N., Hirano H., Mito A. (2019) Unconstrained Vital Sign Monitoring System Using an Aortic Pulse Wave Sensor. *Sci Rep*, 9, 17475.

Haraldsson P. O., Carenfelt C., Laurell H. and Törnros J. (1990) Driving vigilance simulator test. *Acta oto-laryngologica*, 110(1-2), 136–140.

Hayami T., Katsuya M. (2002) Detecting drowsiness while driving by measuring eye movement—A pilot study. *Proceedings of the IEEE 5th International Conference on Intelligent Transportation Systems*, Singapore.

Herman J., Kafoa B., Wainiqolo I., Robinson E., McCaig E., Connor J., Jackson R. and Ameratunga S. (2014) Driver sleepiness and risk of motor vehicle crash injuries: a population-based case control study in Fiji (TRIP 12). *Injury*, 45 (3), 586-591.

Hirsch J. A. and Bishop B. (1981) Respiratory sinus arrhythmia in humans: how breathing pattern modulates heart rate. *The American journal of physiology*, 241(4), H620–H629.

Horne J., Reyner L. (1999) Vehicle accidents related to sleep: a review. *Occup Environ Med*., 56(5), 289–294.

Horrey W.J., Noy Y.I., Folkard S., Popkin S.M., Howarth H.D. and Courtney T.K. (2011) Research needs and opportunities for reducing the adverse safety consequences of fatigue. *Accident Analysis & Prevention*, 43, 591-594.

Houle M.S., Billman G.E. (1999) Low-frequency component of the heart rate spectrum: a poor marker of sympathetic activity. *Am J Physiol Heart Circ Physiol*, 276, 215–23.

Isnainiyah I.N., Samopa F., Suryotrisongko H. and Riksakomara E. (2015) Analysis of sleep deprivation effect to driving performance using reaction test simulation. *Jurnal Teknologi*, 72(4), 61-66.

Jamroz K., Smolarek L. (2013) Driver fatigue and road safety on Poland's national roads. *International Journal of Occupational Safety and Ergonomics*, 19(2), 297-309.

Jiao K., Li Z.Y., Chen M., Wang C.T., Qi S.H. (2004) Effect of different vibration frequencies on heart rate variability and driving drowsiness in healthy drivers. *Int. Arch. Occup. Environ. Health*, 77, 205–212.

Johns M. W., Chapman R., Crowley K. and Tucker A. (2008) A new method for assessing the risks of drowsiness while driving. *Somnologie*, 12, 66–74.

Johns M.W. (2000) A sleep physiologist's view of drowsy driving. *Transportation Research* Part F, 3, 241-249.

Juki: A drowsy driving warning device "SleepBuster," http://www.juki.co.jp/sleepbuster/sleep-buster/sleep-buster.html, accessed March 17, 2014.

Jung S.J., Shin H.S., Chung W.Y. (2014) Driver fatigue and drowsiness monitoring system with embedded electrocardiogram sensor on steering wheel. *IET Intell. Transp. Syst.*, 8, 43–50.

Jurysta F., van de Borne P., Migeotte P.-F., Dumont M., Lanquart J.-P., Degaute J.-P. and Linkowski P. (2003) A study of the dynamic interactions between sleep EEG and heart rate variability in healthy young men. *Clinical Neurophysiology*, 114(11), 2146–2155.

Karmakar C.K., Gubbi J., Khandoker A.H., Palaniswami M. (2010) Analyzing temporal variability of standard descriptors of Poincaré plots. *J. Electrocardiol.*, 43, 719–724.

Kecklund G., Anund A., Rodling Wahlström M., Philip P. and Åkerstedt T. (2011) Sleepiness and the risk of car crash: a case control study, Linköping.

King D.J., Siegmund G.P., Montgomery D.T. (1994) Outfitting a Freightliner Tractor for Measuring Driver Fatigue and Vehicle Kinematics During Closed-Track Testing. Technical Report, *SAE Technical Paper 942326*, Warrendale, PA, USA.

Kleiger R.E., Stein P.K., Bosner M.S., Rottman J.N. (1995) Time domain measurements of heart rate variability. *In:* Malik M, Camm AJ, editors. Heart rate variability. Armonk, N.Y.: Futura Publ. Comp., Inc., 33–45.

Kojima S., Maeda S., Uchikawa R., Nobuhiro Y., Aoi K., Ogura Y., Fujita E., Murata K., Kamei T., Tsuji T., Yoshizumi M., Kaneko S. (2015) Development of a simple system to sense vital signs from the back. *Japan Society of Design Engineering*, Voi. SO, 2, 78-88.

Kribbs N., Dinges D. F. (1994) Vigilance decrement and sleepiness. *In:* Harsh J, Ogilvie R, editors. *Sleep onset mechanisms*. Washington, DC: American Psychological Association, 113-125.

Lajunen T., Parker D., Summala H. (2004) The Manchester driver behaviour questionnaire: a cross-cultural study. *Accident Analysis & Prevention*, 36(2), 231-238.

Lal S.K.L. and Craig A. (2001) A critical review of the psychophysiology of driver fatigue. *Biological Psychology*, 55, 173-194.

Laurin A., Blaber A., Tavakolian K. (2013) Seismocardiograms return valid heart rate variability indices. *In: Proceedings of the Computing in Cardiology 2013*, Zaragoza, Spain, 413–416.

Lee B. G., Jung S. J., Chung W.Y. (2011) Real-time physiological and vision monitoring of vehicle driver for non-intrusive drowsiness detection. *IET Commun.*, 5(17), 2461–2469.

Lee H.B., Choi J.M., Kim J.S., Kim Y.S., Baek H.J., Ryu M.S., Sohn R.Y. and Park K.S. (2007) Nonintrusive Biosignal Measurement System in a Vehicle. *Proceedings of the 29th Annual International Conference of the IEEE EMBS Cite Internationale*, Lyon, France.

Lee S. T., Hon E. H. (1965) The fetal Electrocardiogram. IV. Unusual Variations in the QRS Complex during labor. *American journal of obstetrics and gynecology*, 92, 1140–1148.

Lenskiy A.A., Lee J.S. (2012) Driver's eye blinking detection using novel color and texture segmentation algorithms. *Int. J. Control Autom. Syst.*, 10, 317–327.

Li G. and Chung W. Y. (2013) Detection of driver drowsiness using wavelet analysis of heart rate variability and a support vector machine classifier. *Sensors (Basel, Switzerland)*, 13(12), 16494–16511.

Li G. and Chung W.Y. (2015) A context-aware EEG headset system for early detection of driver drowsiness. Sensors, 15, 20873–20893.

Liang W., Yuan J., Sun D., Lin M. (2009) Changes in physiological parameters induced by indoor simulated driving: Effect of lower body exercise at mid-term break. *Sensors*, 9, 6913–6933.

Litvack D. A., Oberlander T. F., Carney L. H., Saul J. P. (1995) Time and frequency domain methods for heart rate variability analysis: a methodological comparison. *Psychophysiology*, 32, 492–504.

Luczak H. and Laurig W. (1973) An analysis of heart rate variability. *Ergonomics*, *16*(1), 85–97.

Lyznicki J. M., Doege T. C., Davis R. M. and Williams M A. (1998) Sleepiness, driving, and motor vehicle crashes. *Journal of the American Medical Association*, 279(23), 1908- 1913.

Mahachandra M., Yassierli, Sutalaksana, I.Z., Suryadi K. (2012) Sensitivity of Heart Rate Variability as Indicator of Driver Sleepiness. In: *Proceedings of the 2nd International Conference of the South East Asian Network of Ergonomics Societies*, Langkawi, Malaysia, 1–6.

Malik M., Bigger J. T., Camm A. J., Kleiger R. E., Malliani A., Moss A. J., Schwartz P. J. (1996) Heart rate variability: Standards of measurement, physiological interpretation, and clinical use. *European Heart Journal*, 17(3), 354–381.

Malliani A., Lombardi F., Pagani M., Cerutti S. (1994) Power spectral analysis of cardiovascular variability in patients at risk for sudden cardiac death. *J Cardiovasc Electrophysiol*, 5, 274–86.

Massala G.L. and Grosso E. (2014) Real time detection of driver attention: Emerging solutions on robust iconic classifiers and dictionary of poses. *Transportation Research Part C*, 49, 32-42.

Mbouna R. O., Kong S. G. and Chun M. (2013) Visual analysis of eye state and head pose for driver alertness monitoring. *IEEE Transactions on Intelligent Transportation Systems*, 14(3), 1462–1469.

McDonald A. D., Schwarz C., Lee J. D. and Brown T. L. (2012) Real-time detection of drowsiness related lane departures using steering wheel angle. *Proc. Human Factors and Ergonomics Society Annual Meeting*, 56, 2201−2205.

Minjie W., Ping M., Caiyan Z. (2013) Driver fatigue detection algorithm based on the states of eyes and mouth. *Comput. Appl. Softw.*, 30, 25–21.

Miyaji M., Kawanaka H., Oguri, K. (2009) Driver's Cognitive Distraction Detection Using Physiological Features by the Adaboost. *In: Proceedings of the 12th International IEEE Conference on Intelligent Transportation Systems*, St. Louis, MO, USA, 1–6.

Montano N., Porta A., Cogliati C., Costantino G., Tobaldini E., Casali K.R., Iellamo F. (2009) Heart rate variability explored in the frequency domain: A tool to investigate the link between heart and behavior. *Neurosci. Biobehav. Rev.*, 33, 71–80.

Murata K., Fujita E., Kojima S., Maeda S., Ogura Y., Kamei T., Tsuji T., Kaneko S., Yoshizumi M., Suzuki N. (2011) Noninvasive biological sensor system for detection of drunk driving. *IEEE Transactions on ln formation Technology in BioMedicine*, 15(1), 19- 25.

Nagai F., Omi T. and Komura T. (2008) Driver sleepiness detection by video image processing. *FISITA 2008 World Automotive Congress*, Munich, Germany, paper F2008-08-037.

Nishiyama J., Kinoshita S. and Hirata Y. (2010) Prediction of drowsiness by the vestibulo-ocular reflex. *Transactions of the Japanese Society for Medical and Biological Engineering*, 48(1), 1–10.

Ochiai N. (2006) The Application to Fatigue and Sleep Prediction of The Signal of Biological Fluctuation Measured from Noninvasive Sensor. *In: 39" Japan Ergonomics Society Chugoku and Shikoku Branch convention*, Collection of Literatures and Papers, Japan Ergonomics Society Chugoku and Shikoku Branch Secretariat.

Oron-Gilad T., Ronen A. and Shinar D. (2008) Alertness maintaining tasks (AMTs) while driving. *Accident Analysis & Prevention*, 40 (3), 851-860.

Papadelis C., Chen Z., Kourtidou-Papadeli C., Bamidis P.D., Chouvarda I., Bekiaris E. and Maglaveras N. (2007)Monitoring sleepiness with on-board electrophysiological recordings for preventing sleep-deprived traffic accidents. *Clinical Neurophysiology*, 118 (9), 1906-1922.

Patel M., Lal S.K.L., Kavanagh D., Rossiter P. (2011) Applying neural network analysis on heart rate variability data to assess driver drowsiness. *Exp. Syst. Appl.*, 38, 7235–7242.

Philip P., Chaufton C., Orriols L. (2014) Complaints of Poor Sleep and Risk of Traffic Accidents: A Population-Based Case-Control Study. *PLoS One*, 9(12), e114102.

Philip P., Sagaspe P., Moore N., Taillard J. Charles A., Guillleminault C. and Bioulac B.(2005) Fatigue, sleep restriction and driving performance. *Accident Analysis and Prevention*, 37, 473-478.

Picot A., Charbonnier S., Caplier A. (2010) Drowsiness detection based on visual signs: Blinking analysis based on high frame rate video. In: *Proceedings of the 2010 IEEE Instrumentation and Measurement Technology Conference (I2MTC)*, Austin, TX, USA.

Picot A., Charbonnier S., Caplier A. (2012) On-line detection of drowsiness using brain and visual information. *IEEE Trans. Syst. Man Cybern. Part A Syst. Hum.*, 42, 764–775.

Ponikowski P., Chua T.P., Amadi A.A., Piepoli M., Harrington D., Volterrani M. (1996) Detection and significance of a discrete very low frequency rhythm in RR interval variability in chronic congestive heart failure. *Am J Cardiol*, 77, 1320.

Porges S.W. (1995) Cardiac vagal tone: a physiological index of stress. *Neurosci Biobehav Revev*, 19, 225–34.

Porges S.W. (2003) The polyvagal theory: phylogenetic contributions to social behavior. *Physiol Behav*, 79, 503–13.

Pumprla J., Howorka K., Groves D., Chester M., Nolan J. (2002) Functional assessment of heart rate variability: Physiological basis and practical applications. *Int. J. Cardiol.*, 84, 1–14.

Reyner L.A. and Horne J.A. (1998) Falling asleep whilst driving: are drivers aware of prior sleepiness? *International Journal of Legal Medicine*, 111(3), 120–123.

Sagaspe P., Taillard J., Bayon V., Lagarde E., Moore N., Boussuge J., Chaumet G., Bioulac B. and Philip P. (2010) Sleepiness, near-misses and

driving accidents among a representative population of French drivers. *Journal of sleep research*, 19(4), 578–584.

Sagberg F. (1999) Road accidents caused by falling asleep. *Accident Analysis and Prevention*, 31, 639-649.

Sagberg F., Jackson P., Krüger H., Muzet A., Williams A. (2004) Fatigue, Sleepiness and Reduced Alertness as Risk Factors in Driving. *In: Institute of Transport Economics*, Oslo, Norway.

Sahayadhas A., Sundaraj K., Murugappan, M. (2012) Detecting driver drowsiness based on sensors: A review. *Sensors*, 12, 16937–16953.

Salvati L., d'Amore M., Fiorentino A., Pellegrino A., Sena P., Villecco F. (2020) Development and Testing of a Methodology for the Assessment of Acceptability of LKA Systems. *Machines*, 8(3), 47.

Salvati L., d'Amore M., Fiorentino A., Pellegrino A., Sena P., Villecco F. (2021) On-Road Detection of Driver Fatigue and Drowsiness during Medium-Distance Journeys. *Entropy (Basel)*, 23(2), 135.

Santhi N., Horowitz T. S., Duffy J. F., Czeisler C. A. (2007) Acute sleep deprivation and circadian misalignment associated with transition onto the first night of work impairs visual selective attention. *PLoS One*, 2(11), e1233.

Schagen, I.N.L.G.van (2003) Vermoeidheid achter het stuur. Report 2003-16, Institute for Road Safety Research SWOV, Netherlands, Leidschendam Accessed 15 January 2008: http://www.swov.nl/rapport/R-2003-16.pdf.

Serrador J. M., Finlayson H. C., Hughson R. L. (1999) Physical activity is a major contributor to the ultra low frequency components of heart rate variability. *Heart*, 82(6).

Shin H.S., Jung S.J., Kim J., Chung W.Y. (2010) Real Time Car Driver's Condition Monitoring System. In: *Proceedings of IEEE Sensors Conference*, Waikoloa, HI, USA, 951–954.

Slater J. D. (2008) A definition of drowsiness: One purpose for sleep? *Med. Hypotheses*, 71, 641–644.

Sun Y. and Yu X. (2014) An Innovative Non-intrusive Driver Assistance System for Vital Signal Monitoring. IEEE, *Journal of Biomedical and Health Informatics*, 18(6), 1932 – 1939.

Tadi M.J., Lehtonen E., Koivisto T., Pänkäälä M., Paasio A., Teräs M. (2015) Seismocardiography: Toward heart rate variability (HRV) estimation. In: *Proceedings of the 2015 IEEE International Symposium on Medical Measurements and Applications (MeMeA) Proceedings*, Turin, Italy, 261–266.

Thompson J., Stevenson M. (2014) Associations between heavy-vehicle driver compensation methods, fatigue-related driving behavior, and sleepiness. *Traffic Injury Prevention*, 15(S1), 10-14.

Tianyi M.A., Cheng B. (2010) Detection of driver's drowsiness using facial expression features. *J. Automot. Saf. Energy*, 1, 200-204.

Tobaldini E., Nobili L., Strada S., Casali K. R., Braghiroli A. and Montano N. (2013) Heart rate variability in normal and pathological sleep. *Frontiers in Physiology*, 4, 294.

Townsend R., Wilkinson I., Schiffrin E., Avolio A., Chirinos J., Cockcroft J. (2015) Recommendations for Improving and Standardizing Vascular Research on Arterial Stiffness: A Scientific Statement from the American Heart Association. *Hypertension*, 66(3), 698–722.

Treat J. R., Tumbas N. S., McDonald S. T., Shinar D., Hume R. D., Mayer R. E., Stansifer R. L., Castellan N. John (1977) *Tri-level study of the causes of traffic accidents: final report. Volume I: causal factor tabulations and assessments.*

Trinder J., Kleiman J., Carrington M., Smith S., Breen S., Tan N. and Kim Y. (2001) Autonomic activity during human sleep as a function of time and sleep stage. *Journal of sleep research*, 10(4), 253–264.

Van Dongen H. P., Maislin G., Mullington J. M., Dinges D. F. (2003) The cumulative cost of additional wakefulness: dose-response effects on neurobehavioral functions and sleep physiology from chronic sleep restriction and total sleep deprivation. *Sleep*, 26(2), 117-126.

Versace F., Mozzato M., De Min Tona G., Cavallero C., Stegagno (2003) L. Heart rate variability during sleep as a function of the sleep cycle. *Biological Psychology*, 63(2), 146–162.

Vitabile S., Paola A.D., Sorbello F. (2011) A real-time non-intrusive FPGA-based drowsiness detection system. *J. Ambient Intell. Humaniz. Comput.*, 2, 251–262.

von Borell E., Langbein J., Després G., Hansen S., Leterrier C., Marchant-Forde J., Marchant-Forde R., Minero M., Mohr E., Prunier A., Valance D., Veissier I. (2007) Heart rate variability as a measure of autonomic regulation of cardiac activity for assessing stress and welfare in farm animals -- a review. *Physiol Behav.*, 92(3), 293-316.

WHO (2011) Global Plan for the Decade of Action for road Safety 2011-2020, Geneva.

Wierwille W.W., Ellsworth L.A., Wreggit S.S., Fairbanks R.J., Kirn C.L. (1994a) Research on Vehicle-Based Driver Status/Performance Monitoring Development, Validation, and Refinement of Algorithms for Detection of Driver Drowsiness. Technical Report DOT HS 808 247, Office of Crash Avoidance Research National Highway Traffic Safety Administration, Washington, DC, USA, 23 December.

Wierwille, W. W. and Ellsworth, L. A. (1994b). Evaluation of driver drowsiness by trained raters. *Accident Analysis and Prevention*, 26(5), 571.

Wierwille W.W., Lewin M.G., Fairbanks R.J. (1996) Research on Vehicle-Based Driver Status/performance Monitoring. Technical Report, *The National Academies of Sciences, Engineering, and Medicine*, Washington, DC, USA.

Williamson A., Friswell R., Olivier J. (2014) Are drivers aware of sleepiness and increasing crash risk while driving? *Accident Analysis & Prevention*, 70(5), 225-234.

Wolf J. A. and Rubinstein L. M. (1977) Safety of prostaglandin F2alpha in abortion. *American journal of obstetrics and gynecology*, *129*(8), 928–929.

Wright N.A., Stone B.M., Horberry T.J. and Reed N. (2007) A review of in-vehicle sleepiness detection devices. *TRL Limited*, Published Project Report PPR157.

Yang G.S., Lin Y.Z., Bhattacharya P. (2010) A driver drowsiness recognition model based on information fusion and dynamic Bayesian network. *Inf. Sci.*, 180, 1942–1954.

Yang J. H., Mao Z., Tijerina L., Pilutti T., Coughlin J. F. and Feron E. (2009) Detection of Driver Fatigue Caused by Sleep Deprivation in *IEEE Transactions on Systems, Man, and Cybernetics - Part A: Systems and Humans*, 39(4), 694-705.

Yeragani V.K., Rao R., Jayaraman A., Poh R., Balon R., Glitz D. (2002) Heart rate time series: decreased chaos after intravenous lactate and increased nonlinearity after isoproterenol in normal subjects. *Psychiatry Res*, 109, 81–92.

Zhang C., Wang H., Fu, R. (2014) Automated detection of driver fatigue based on entropy and complexity measures. *IEEE Trans. Intell. Transp. Syst.*, 15, 168–177.

La borsa di dottorato è stata cofinanziata con risorse del
Programma Operativo Nazionale Ricerca e Innovazione 2014-2020 (CCI 2014IT16M2OP005),
Fondo Sociale Europeo, Azione I.1 "Dottorati Innovativi con caratterizzazione Industriale"

UNIONE EUROPEA
Fondo Sociale Europeo